frontiers | Frontiers in Environmental Archaeology

TYPE Original Research
PUBLISHED 06 July 2023
DOI 10.3389/fearc.2023.1206750

OPEN ACCESS

EDITED BY
Francesco Berna,
Simon Fraser University, Canada

REVIEWED BY
Dario Gioia,
Institute of Cultural Heritage Sciences (CNR), Italy
Daniel Alexander Contreras,
University of Florida, United States

*CORRESPONDENCE
Gian Battista Marras
✉ gbm27@cam.ac.uk

RECEIVED 16 April 2023
ACCEPTED 06 June 2023
PUBLISHED 06 July 2023

CITATION
Marras GB and Boschian G (2023) Neolithic settlement and paleopedological changes during the Middle Holocene in northern Sardinia (Italy).
Front. Environ. Archaeol. 2:1206750.
doi: 10.3389/fearc.2023.1206750

Neolithic settlement and paleopedological changes during the Middle Holocene in northern Sardinia (Italy)

Gian Battista Marras[1]* and Giovanni Boschian[2,3]

[1]Department of Archaeology, University of Cambridge, England, United Kingdom, [2]Department of Biology, University of Pisa, Pisa, Italy, [3]Palaeo-Research Institute, University of Johannesburg, Johannesburg, South Africa

Sardinia is the second biggest island in the Mediterranean region and has been intensely settled since the Middle Holocene (c.7750 BP). Despite a large number of documented Neolithic archaeological sites, very little is known about human-environmental interactions, including land use and domestic activities associated with the emergence and expansion of Neolithic settlements (c. 7750 and 5500 BP). To shed new light on these issues, we carried out new geoarchaeological analyses on buried soils and archaeological sequences exposed at the Neolithic site of Contraguda, northern Sardinia. Physical-chemical analyses combined with a micromorphological study of 24 thin sections from archaeological deposits and buried soil horizons were performed to evaluate the formation processes of archaeological deposits and paleosols. Soil micromorphology detected the presence of pedofeatures originating from land clearance and agricultural activities from the buried Vertisol. Vertisol and Entisol formation largely resulted from the anthropic impact on the landscape, which changed the trajectories of soil development and caused desertification of the environment. Furthermore, sediment fabric and pedofeatures also allowed us to reconstruct Neolithic domestic practices, showing that household maintenance waste debris, which also included animal penning refusal, was dumped into pit structures. Together, our results provide the first geoarchaeological evidence of human impact on soil development within the island during the Middle Holocene and give new insight into the Middle Neolithic (c. 6500-6000 BP) domestic behaviour and land use activities. These findings have significant implications for understanding the island's pedological history and offer a valuable insight on the settlement organization of the Neolithic farming communities and their impacts on the paleoenvironment of Sardinia.

KEYWORDS

middle Neolithic land use, soil micromorphology, anthropogenic landscape transformations, household deposits, Sardinia (Western Mediterranean), paleoenvironment, soils, geoarchaeology

1. Introduction

For more than 50 years, research has focused on understanding and disentangling the roles of people and climatic impacts in driving landscape changes in the Mediterranean region during the last 11,700 years (e.g., Vita-Finzi, 1969; Barker, 1995; Roberts, 2014; Roberts et al., 2019). Soils, particularly those that have been buried beneath sediment accumulations (paleosols), have been used in different contexts to investigate and reconstruct the processes of landscape evolution linked with vegetational, climatic, and societal changes (e.g., Fedoroff and Goldberg, 1982; Fedoroff et al., 1990; Catt, 1991; Butzer, 2005; French et al., 2009). Soil micromorphology, by studying the organization and composition

of sediments and soils in thin sections, enables the reconstruction of the origin, the depositional, and post-depositional processes of sedimentary units, and allows researchers to infer more robust interpretations than those made by the naked eye in the field (Goldberg et al., 2009). In addition, it has been widely applied across the Mediterranean region and European continental areas to reconstruct sequences of soil and environmental change in relationship to the identification of past land use practices (e.g., Courty et al., 1989; Macphail et al., 1990; Thompson et al., 1990; Spek et al., 2003; French, 2005; Lewis, 2012; Nielsen and Dalsgaard, 2017; Nielsen et al., 2019). The juxtaposition of soil materials from surface and subsurface soil horizons, compaction and compression features at the base of the plow zone, together with the formation of surface crusts and the translocation of fine materials through voids are all direct and indirect micromorphological indicators of soil subjected to agricultural impacts (Deák et al., 2017; French, 2022). A Mediterranean instance of Middle Holocene soil changes related to prehistoric impact is that of the Gozo Island in the Maltese archipelago, where existed a brown-forest soil buried beneath the Neolithic temple monuments with features such as strong oxidation, secondary calcium carbonate, and a fine organic/charcoal dust indicated that prehistoric disturbance was turning them into Red Mediterranean xeric soils (French et al., 2018). However, in Sardinia, the second biggest island in the Mediterranean basin, indications of paleoenvironmental change inferred from the study of paleosols and their interactions with past human impact and climate conditions are still few and far from providing a complete picture (Boschian, 2003; Vingiani et al., 2004; Carboni et al., 2006; Scarciglia et al., 2011; Nicosia et al., 2013; Zucca et al., 2013; French et al., 2016). For example, Nicosia et al. (2013) reconstructed an environmental sequence of woodland clearance, cultivation, and forest regeneration after human abandonment based on the superimposition of textural pedofeatures along the paleosols across a Late Holocene Punic farmstead on the central-western coast of Sardinia.

Building on and expanding from previous research, this work focuses on the use of soil micromorphological and physical-chemical analyses to define the landscape evolution processes and to decipher the links between prehistoric settlement, soilscape, environmental conditions, and climate changes in the paleopedological and archaeological records of the Contraguda hill, northern Sardinia, in the Middle Holocene period (Figure 1A).

After two millennia of episodic Mesolithic frequentation of the island's coasts, Sardinia has been intensely settled since ca. 7750 BP, when Early Neolithic Cardiale Ware communities colonized the region (Lugliè, 2018). Around 7000 years BP, important developments corresponded to the onset of the *Bonu Ighinu* Middle Neolithic-A phase, which is associated with the earliest hypogeic tomb in the western Mediterranean (Santoni, 2000; Sebis et al., 2012). Developing from this cultural aspect, the *San Ciriaco facies* or Middle Neolithic-B, represented by a highly standardized pottery style, spread across the island. It was associated with open-air farming settlements, and with a pervasive circulation of central-western Sardinia obsidian throughout the north-western Mediterranean basin (Lugliè, 2009, 2012; Binder et al., 2012; Fanti et al., 2018). From 6000 to ca. 5500 BP, the island was characterized by the spread of the Late Neolithic *Ozieri* cultural aspect, which featured the rise of rock-cut tombs, whose rectangular modules resembled the open-air house structures (Robin et al., 2022). It eventually gave way to the Early Copper Age culture called *Sub-Ozieri* (Melis, 2013).

Despite the high number of archaeological sites, very little is known about the interaction of different Neolithic cultural aspects with past soil-environment conditions of the island, and the connections between climate and anthropic factors in driving past landscape changes. The present-day climatic conditions of northern Sardinia are characterized by a temperate warm climate featuring an average annual temperature of 16°C and 500 to 800 mm of annual rainfall (Pinna, 1954). This is associated with spontaneous vegetation of the Mediterranean maquis, with oak woodland stands occurring in the moister zones, and marked by widespread farmlands and pasture lands (Pinna, 1954). On the other hand, the region lacks any paleoclimate reconstruction for the Holocene period, hindering the understanding of the interactions between past environmental conditions, climate change, and human impact. However, different fossil pollen sequences highlighted that the vegetational cover across the island was dominated by shrubland taxa for most of the Middle Holocene period, until ca. 5000 BP when evergreen oak forests expanded at the expense of shrubs such as *Erica spp*. (Di Rita and Melis, 2013; Beffa et al., 2016; Melis et al., 2018; Pedrotta et al., 2021). Nevertheless, the understanding of this vegetational turnover is still poorly understood, while increasing evidence from nearby Corsica suggests that Neolithic land use was a fundamental driving factor (e.g., Revelles et al., 2019; Di Rita et al., 2022).

Here, we present the results of soil micromorphological and physical-chemical analyses carried out on paleosols and archaeological deposits dated to 6300–5700 cal BP at the Contraguda hill, northern Sardinia. Accordingly, a major phase of anthropogenic landscape transformation occurred on the site due to the expansion of the Middle Neolithic-B settlement, leading to a significantly degraded environment, already when Late Neolithic groups re-occupied the area.

2. The site of contraguda: geological and geoarchaeological summary

The Contraguda hill is a low and rounded hill encompassed in a landscape of gently sloping hills dissected by the northern tributaries of the Riu Altana river, which out-flows on the northern Sardinian coast (Boschian, 2003). Lower Pleistocene terraces sit on the slopes of these hills (Ulzega, 1999). Miocene marls, characterized by alternating laminae of Pteropod fossils and pure clay units interlayered by chert bands, crop out at the top of the Contraguda hill, and are underlain by Oligocene calc-alkaline volcanites (Ulzega, 1999; Boschian, 2003) (Figure 1B). In this part of northern Sardinia, the soilscape of marl hilltops is dominated by a thin soil cover of Lithic Xerorthents with wide areas of rock outcrop, and secondarily by Xerochrepts (Aru et al., 1991).

Here, a summary of the key findings by Boschian and colleagues is presented to frame the analyses conducted in the present work (Boschian et al., 2001; Boschian, 2003; Falchi et al., 2012). A series of pit structures characterized by a fill of stones and artifacts were

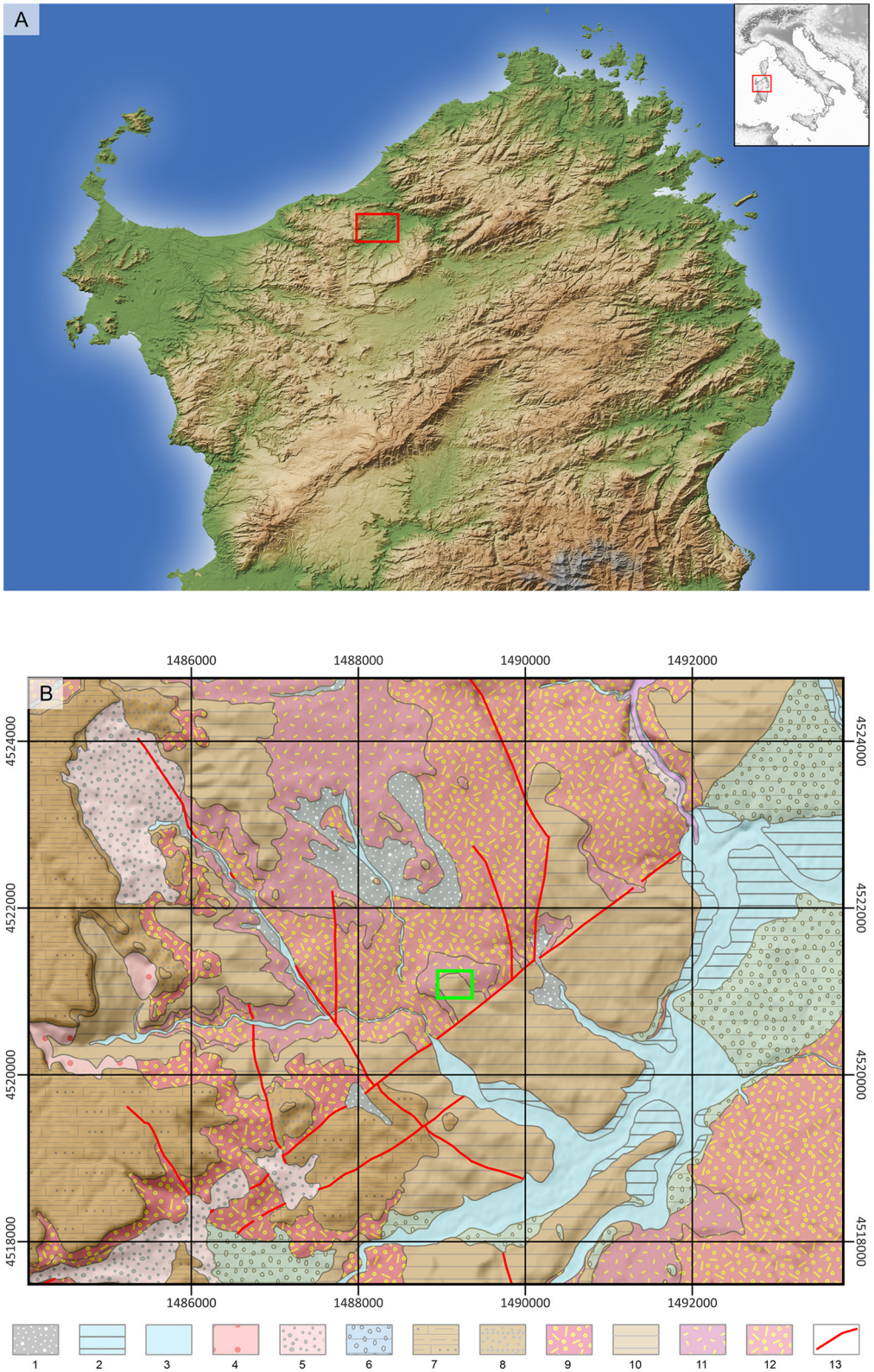

FIGURE 1
(A) Digital Elevation Model of the area around Contraguda (elaboration from 30 m-resolution ALOS Global Digital Surface Model, Japan Aerospace Exploration Agency). Red square: Contraguda hill; **(B)** geological map with the study area indicated in the green box (coordinate system Roma40/Monte Mario W), Holocene: 1 - eluvial and colluvial cover; 2 - river sediments, terraced; 3 - river sediments; 4 - landslide bodies; 5 - scree. Late Pleistocene: 6 - coarse river sediments, terraced. Burdigalian: 7 - calcarenites and bioclastic limestones; 8 - sandstones and conglomerates; 9 - moderately welded ignimbrites (pumice and ash), rhyodacite composition; 10 - lacustrine siltstones and marls with chert beds; 11 - strongly welded ignimbrites (pumice and ash), rhyodacite composition; 12 - strongly welded reddish ignimbrites (pumice and ash); 13 – faults (geological data from: https://www.sardegnageoportale.it/index.php?xsl=2420&s=40&v=9&c=14479&es=6603&na=1&n=100&esp=1&tb=14401).

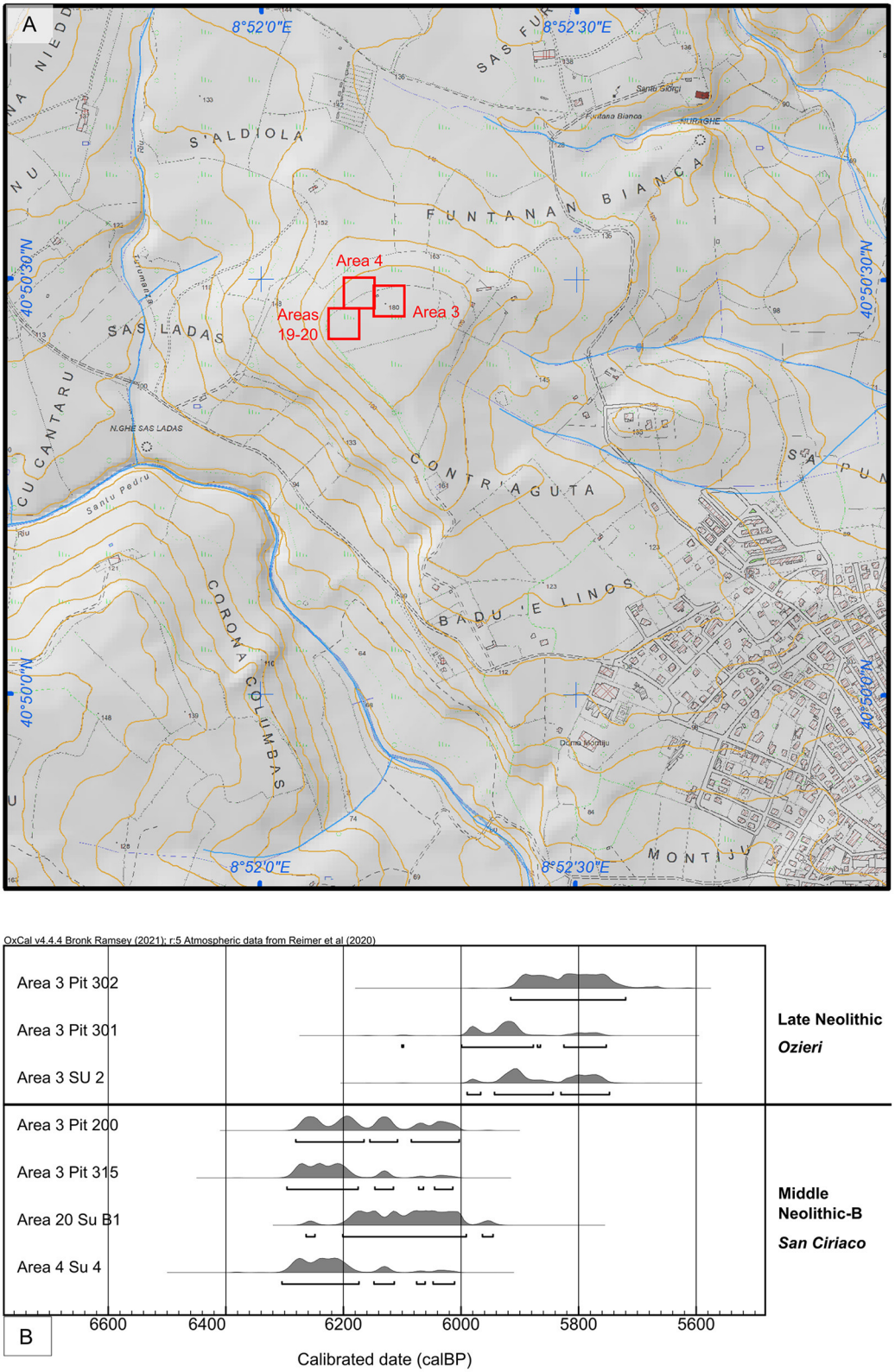

FIGURE 2
(A) Topographic map of the Contraguda hill with highlighted in red the position of the excavation areas; **(B)** re-calibrated dates of the archaeological units and pit structures from the Contraguda hill (position of areas and uncalibrated dates taken from Boschian et al., 2001).

found across the top of the Contraguda hill in four excavated areas, Areas 3, 4, 19, and 20 (Figure 2A). The pottery style and radiocarbon dates from the archaeological deposits suggest that the Neolithic settlement occurred in two periods (Figure 2B). The earliest phase was also the most significant one, to which belong Units 3, 4, 4b, and 5 of Areas 3 and 4, and B, C, D, and DP from Areas 19 and 20. These represent the occupation and the expansion of the Contraguda settlement by the Middle Neolithic-B/*San Ciriaco* communities between 6300 and 6000 cal BP. A second phase was identified in a restricted part of Area 3. Following the pottery style and radiocarbon dates from two pit structures and the archaeological sedimentary Unit 2, it was ascribed to the later and likely episodic occupation by Late Neolithic/*Ozieri* groups, between ca. 6000 and 5700 cal BP.

A vertic paleosol, often truncated by the Middle Neolithic archaeological deposits or buried beneath the present-day Xerorthent soil, was identified during the excavation in Areas 4, 19, and 20. Characteristic pedofeatures, such as Terra-Rossa-like ped fragments, and fragmented clay coatings, suggest a complex pedogenesis that likely started during the Pleistocene and culminated in the vertic processes that promoted the settlement by Neolithic farmers (Limbrey, 1990). Furthermore, a poorly developed calcic paleosol associated with Late Neolithic artifacts was found only in Area 3. Particularly in this part of the hilltop, the archaeological deposits lie directly on the marly bedrock, suggesting that marked soil loss and erosion processes occurred during the prehistoric occupation of the Contraguda hill.

The results summarized here revealed a significant reconstruction of the human-environmental interactions in northern Sardinia during the Neolithic period. However, they also leave some fundamental questions open. Which were the formation processes of the archaeological deposits found at Contraguda? What is the soil forming history of the Contraguda soilscape, and by extent, of the northern Sardinia hilltop soils? How was land used, and what was the role of the Middle and Late Neolithic settlements in driving past landscape transformations?

3. Materials and methods

Undisturbed samples were collected in different excavation seasons by one of us (Boschian in 1997 and 1998; Table 1). Block samples were taken at different depths by carving out soil and sediment blocks and wrapping them tightly with cellulose paper and masking tape. Thin sections measuring 90 × 55 mm were manufactured from these samples at the Massimo Sbrana Laboratory for Geological Services (Piombino, IT). The micromorphological analysis was carried out using Leica Laborlux 12 Pol petrographic microscope at x4, x10, and x25 magnifications at the McBurney Laboratory for Geoarchaeology (University of Cambridge, UK), following the reference textbooks for soil micromorphology description and components identification (Bullock et al., 1985; Courty et al., 1989; Stoops, 2003; Nicosia and Stoops, 2017; Stoops et al., 2018; Verrecchia and Trombino, 2021). Together with the undisturbed soil and sediment blocks, bulk samples were collected at different depths to determine $CaCO_3$ percentage, organic Carbon content, and bulk density in almost every sedimentary unit.

TABLE 1 List of micromorphological and bulk samples collected at the site of Contraguda.

Sample number	Area	Sedimentary unit
C2/97/3	4	3
C3/97/PM	4	Entisol
C4/97/4	4	4
C5/97/4b	4	4b
C6/97/PS1	4	Vertisol
C7/97/PS2	4	Vertisol
C8/97/PS3	4	Vertisol
C9/97/2	4	2
C10/97	4	Fill of pit n. 5
C11/97/5	4	5
C12/98/5	3	5
C13/98/PM	4	Entisol
C14/98/B	20	B
C15/98/C	20	C
C16/98/5	3	5
C17/98/4	3	4
C18/98/4	3	4
C19/98/3	3	3
C20/98/5	3	5
C21/98/5	3	5
C22/98/4	3	4
C23/98/3	3	3
C24/98/D	19	D
C25/98/DP	19	DP

4. Results

Below, we describe the results of micromorphological and physical-chemical analyses, presented in three sections divided according to the site areas and their related sedimentary units. Scans and full descriptions of thin sections are provided in the Supplementary material.

4.1. The paleosols from areas 3 and 4

Two paleosols truncated by the archaeological deposits or buried under the present-day soil were identified in Areas 3 and 4 and were grouped within the Entisol and Vertisol orders (Boschian, 2003).

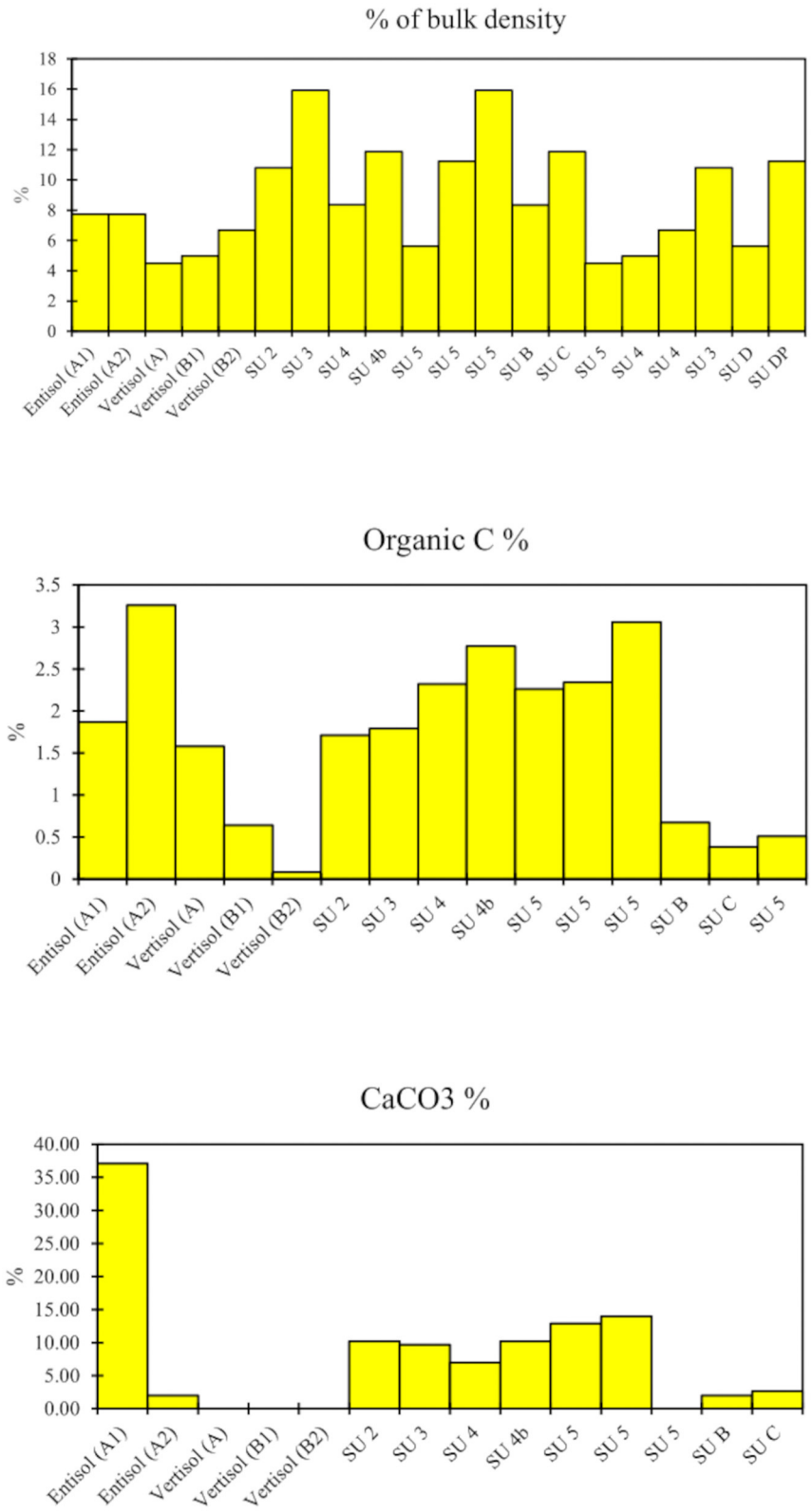

FIGURE 3
Results of the physical-chemical analyses of the lithological units constituting the archaeological deposits and of the buried soil profiles. Buried soil horizons are indicated with their letter in brackets.

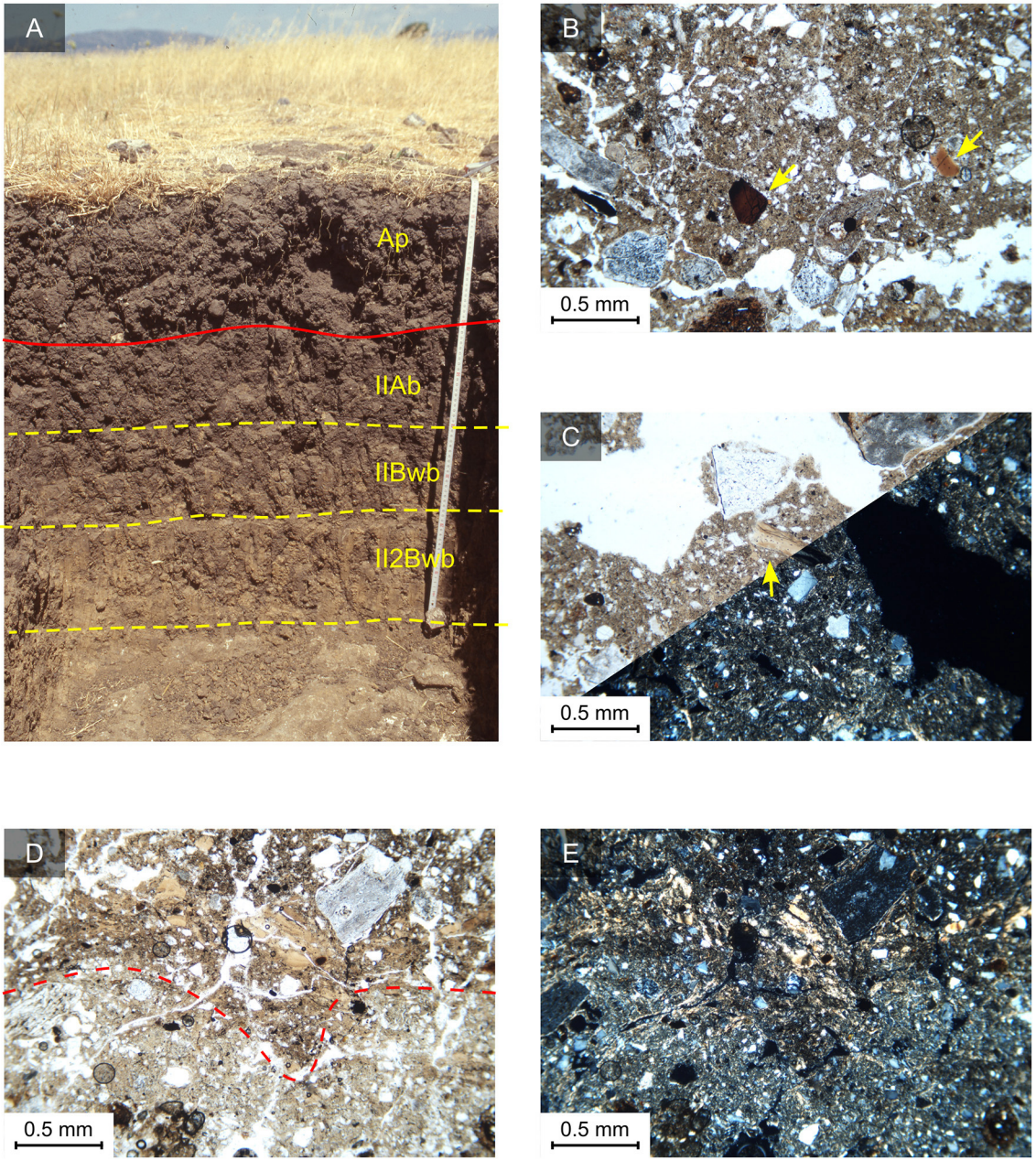

FIGURE 4
(A) The reference Vertisol profile excavated in Area 4, buried under the modern soil under pasture (Boschian, 1998); **(B)** and **(C)** C6/97/PS1 – IIAb horizon, humic fabric and the coarse fraction of volcanic rock fragments, feldspars, and cherts. Indicated by yellow arrows are fresh and burnt bone fragments that could have been added to the soil by Neolithic amendment practices; **(D)** C6/97/PS1 base – IIAb horizon, the transition between the IIAb and IIBwb horizon showing an abrupt wavy boundary (red dashed line) overlain by shear-stress features resulting from the impact of agricultural tools during plowing (e.g., Lewis, 2012; French, 2022), corresponding to the Middle Neolitic-B plow-zone, PPL; **(E)** same as D in XPL, showing a striated B-fabric resulted from mechanical shear stress (e.g., Lewis, 2012; French, 2022).

4.1.1. Physical-chemical parameters

Physical-chemical analyses were carried out on bulk samples taken at different depths from the Vertisol and Entisol of Area 4, allowing a quantitative characterization of the buried soil properties (Figure 3). For instance, samples taken from the Entisol indicate a significant content of calcium carbonate in the upper horizon and a marked decrease in the basal horizon. In contrast, samples from the Vertisol are completely decalcified. The organic C content decreases downwards in the Vertisol profile, while the bulk density increases. In the Entisol profile, the organic carbon is depleted in the upper part compared to the basal horizon, while the bulk density is the same along the profile.

4.1.2. Micromorphology

The characteristics of the two paleosols vary strongly, therefore they are described separately here:

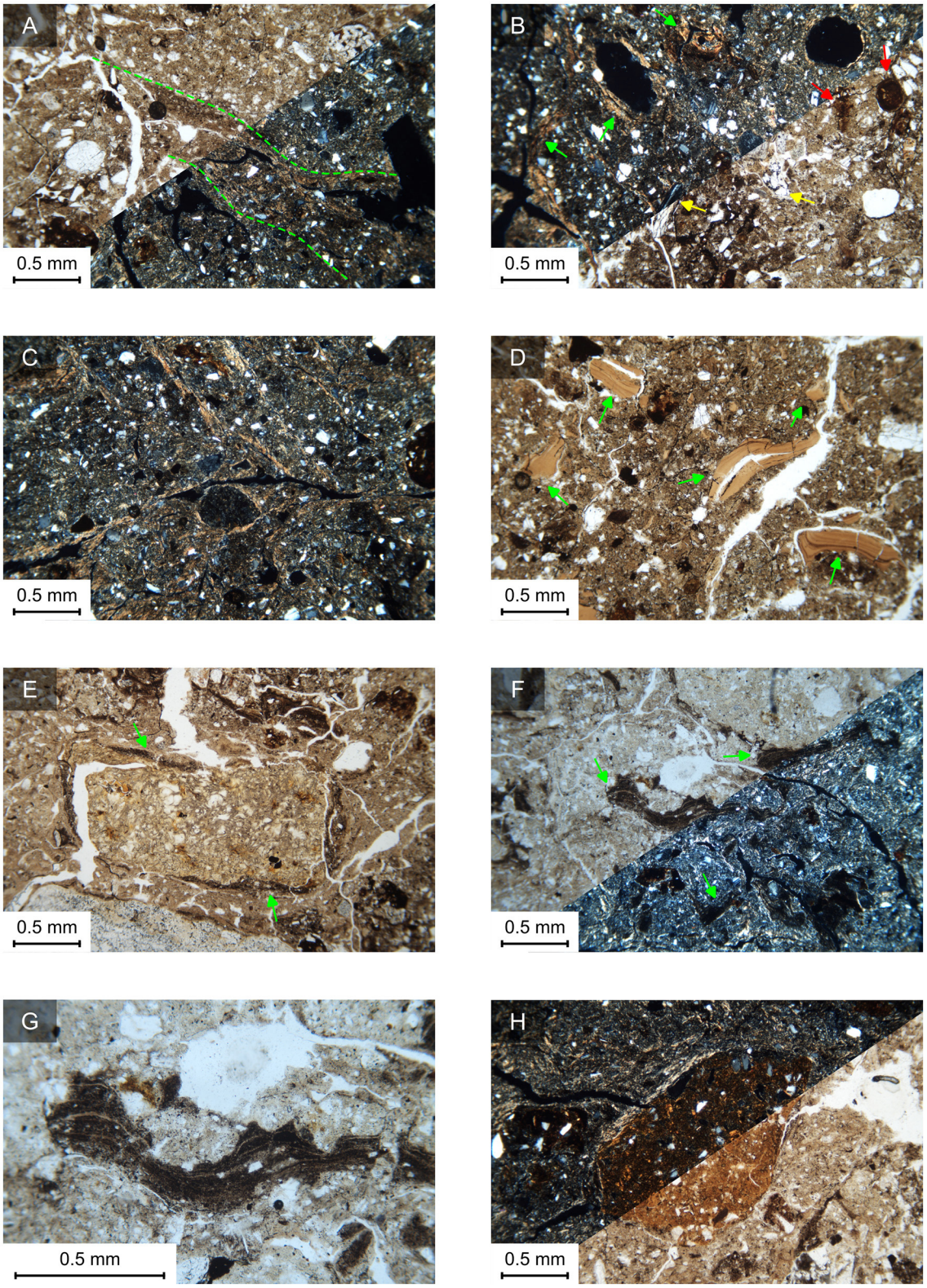

FIGURE 5
(A) C7/97/PS2, top– IIBw horizon, infilling of a channel by non-laminated dirty clay and mineral sand grains, which occurs in cultivated soils with bare plowed surfaces (e.g., Deák et al., 2017; Macphail and Goldberg, 2018), PPL and XPL; **(B)** C7/97/PS2, top– IIBw horizon, intermixed humic and sandy clay loam fabrics in the upper part of the IIBwb horizon, with common dirty clay coatings (green arrows) and bone fragments (yellow arrows), indicating prehistoric soil management and agricultural practices. Also present in the sandy clay loam fabric are *in situ*-formed concentric Fe nodules with diffuse boundaries (red arrows), suggesting rapid and intense drying, PPL and XPL; **(C)** C7/97/PS2, middle-bottom – IIBw horizon, poro- and cross-striation B-fabrics characterizing the B-horizons of the Vertisol, which form due to shrinking-swelling properties, XPL; **(D)** C7/97/PS2, base –
(Continued)

FIGURE 5 (Continued)
IIBw horizon, fragmented and dislodged laminated pure and fine dusty clays, which are relict pedofeatures of a former forest brown soil disrupted by prehistoric deforestation and dispersed in the soil by vertic processes, PPL; **(E)** C8/97/PS3 – II2Bw horizon, *in situ*-formed dirty clay coatings (green arrows) on a large spongy bone fragment, PPL; **(F)** C8/97/PS3 – II2Bw horizon, laminated dirty clay coatings (green arrows) on interpedal channels, formed due to prehistoric vegetation clearance (e.g., Deák et al., 2017; Macphail and Goldberg, 2018), PPL and XPL; **(G)** detail of the laminated dirty clay coating in F, with alternating laminae richer in micro-contrasted dark particles and silt-size sand grains; **(H)** C8/97/PS3 – II2Bw horizon, red clay loam pedorelict found at the base of the Vertisol, indicating the former presence of a Pleistocene Terra Rossa soil on the Contraguda hill, PPL and XPL.

4.1.2.1. Vertisol

Throughout the profile (Figure 4A), the soil displays well-developed angular blocky peds often with pointed edges, separated by straight or zig-zag planes and channels. The groundmass is characterized by a clay loam texture, in which moderately sorted fine sand grains are embedded in a silty clay micromass. However, the upper part is characterized by angular blocky peds with clay loam texture mixed with sandy loam subangular peds, richer in dispersed organic materials. Fine and very fine sands are mainly composed of feldspars, while the coarse grains consist of chert, trachyte fragments, and large feldspar clasts. The micromass shows a markedly striated B-fabric, such as poro-, grano-, and random-striated, that evolves downwards into a more accentuated cross-striation (Figure 5C). Similarly, the organic components vary according to depth. In the upper part, they are more frequent and composed of fragments of plant tissues often found in channels, amorphous organic matter, charcoal, humified vegetal remains, and fresh and burnt bone fragments (Figures 4B, C). Charcoal and bone fragments are the only organic components in the deeper sample. The inorganic elements are represented by isolated phytolith cells, occurring throughout the profile. These have different shapes and margins, mainly of the elongate entire and dentate, star-shaped and bulliform types, but also spheroidal echinate types are found in the basal part. The pedofeatures of this soil are mostly related to different types of textural features and nodule formation. Accordingly, a sequence of superimposed textural pedofeatures can be traced from the basal to upper horizons. Starting from the buried B-horizons, numerous fragments of laminated, well-oriented, limpid to dusty clay coatings (orange-yellow in PPL; bright yellow and dark orange in XPL) are found scattered through the groundmass (Figure 5D). These well-oriented clay coatings are not directly connected with the porosity of the soil, but seem reworked, disrupted, and dislodged from their original sites. On the other hand, *in situ* laminated dirty clay coatings (dark brown in PPL, extinct in XPL) rich in micro-contrasted dark particles are detected at the base of channels or interpedal planes (Figures 5F, G), but also capping soil peds and coating groundmass elements such as bone fragments (Figure 5E). At the base of the buried A-horizon, non-oriented dusty-dirty clay coatings (dark orange brown in PPL, brown speckled orange in XPL) are detected at the base of channels and interpedal voids, mixed with fine sand- and silt-size mineral and organic grains (Figures 5A, B). Furthermore, the transition between the humic A- and the B-horizon is characterized by an abrupt wavy contact showing shear stress-, compression-related features aligned along the base of the A-horizon boundary (Figures 4D, E). Also, different types of Fe-Mn nodules are identified along the whole profile. Amorphous Fe-Mn impregnations are common from the top to the bottom of the soil, often evolving into typic impregnative and concentric nodules characterized by layers of silt and fine sand cemented by sesquioxides. Finally, aggregates resembling relics of Terra Rossa soil, composed of clay loam and well-sorted fine sand (orange under PPL; bright red in XPL), with sharp boundaries, are found predominantly in the basal part of the profile (Boschian, 2003) (Figure 5H).

4.1.2.2. Entisol

Generally, this soil is characterized by poorly developed and poorly separated sub-angular peds and a higher content of detrital and pedogenic carbonates compared to the Vertisol (Figure 6A). The groundmass features moderately sorted medium to fine sand grains mainly composed of plagioclase, K-feldspar, pyroxene, chert, and coarser trachyte fragments. Regarding the micromass, this is constituted of a humic silty clay having an undifferentiated B-fabric. The organic components are fine sand-size charcoal, amorphous organic matter, and fresh and burnt bone fragments (Figure 6B). On the other hand, a fabric richer in carbonates and marl fragments, associated with a calcareous silty clay with crystallitic B-fabric, is found in large channels and disrupted areas among peds with undifferentiated B-fabric (Figures 6B, C). This fabric is also characterized by numerous calcitic pedofeatures. For example, the groundmass is strongly impregnated by micrite. Micrite coatings and hypocoatings were also very common in channels, and some of them can be regarded as calcite pseudomorphs on roots (rhizoliths). On the contrary, the humic groundmass lacks most of the calcium carbonate pedofeatures, whereas only a few incipient micritic impregnative nodules are detected (Figure 6D). Also anthropic artifacts, such as pottery fragments with a rounded shape are randomly mixed with the soil material (Figure 6E).

4.2. The archaeological sequence from areas 3 and 4

A total of 14 samples collected from the archaeological deposits filling the pits excavated in the bedrock in Areas 3 and 4 were analyzed with micromorphological and physical-chemical laboratory techniques.

4.2.1. Physical-chemical parameters

For physical-chemical analyses, bulk samples were taken from different sedimentary units of the archaeological deposits (Figure 6). Generally, these values range in the same spectrum except for Unit 5 from Area 3. All samples from Area 4 have a

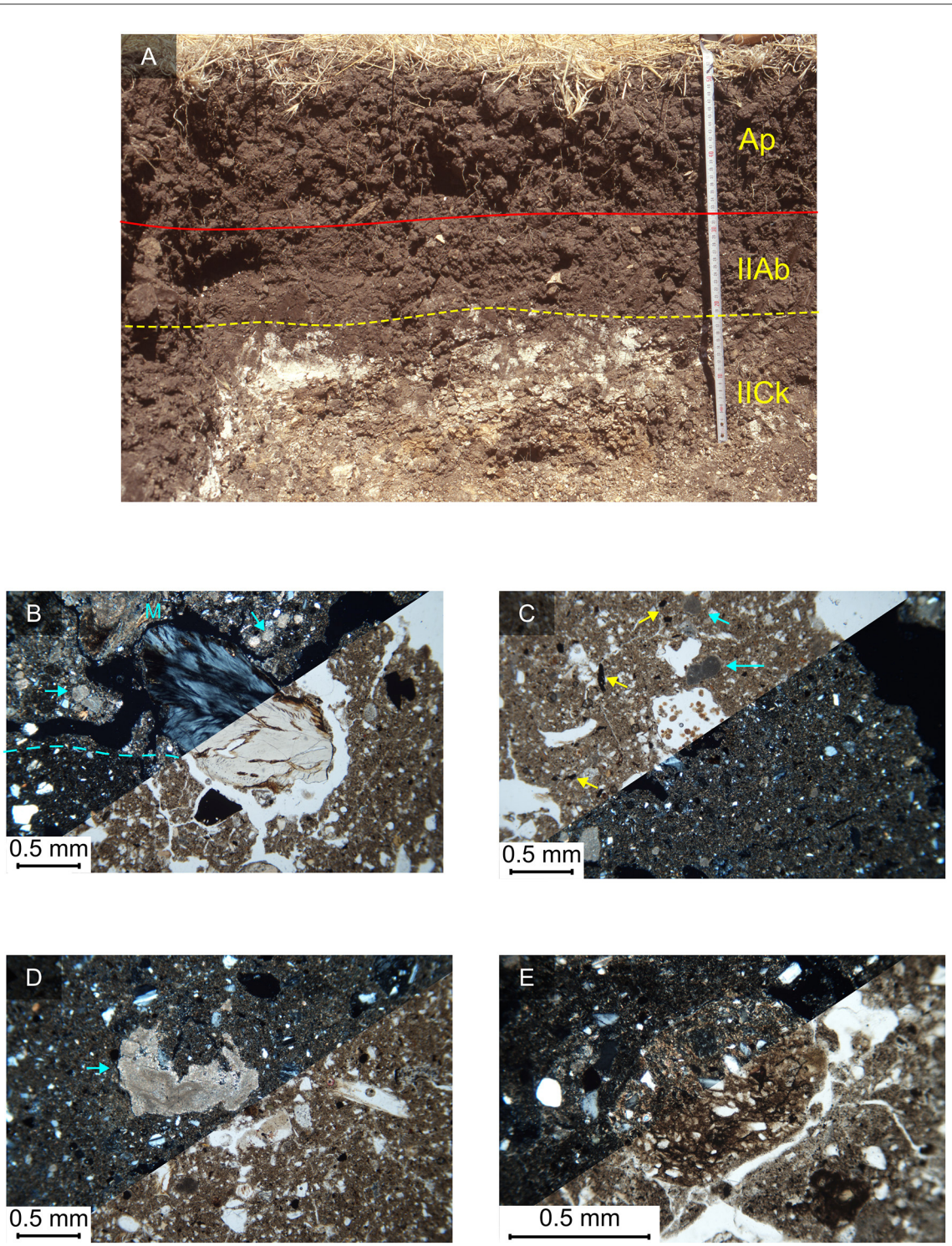

FIGURE 6
(A) reference Entisol profile buried under the modern soil under pasture in Area 3 (G. Boschian); **(B)** C3/97/PM – IIAb, irregularly juxtaposed peds of humic material with a non-calcareous, undifferentiated, groundmass and peds rich in geogenic, such as marl fragments (M), and pedogenic calcium carbonate, like micritic nodules (cyan arrows), indicating recalcification from precipitation of carbonates due to colluvial inputs of weathered marl fragments. A large burnt bone fragment is present in the middle of the frame suggesting some degree of land use linked to the Late Neolithic occupation of the area, inside a channel likely formed due to drying, PPL and XPL; **(C)** C3/97/PM – IIAb horizon, weakly crystallitic B-fabric and humified charcoal fragments (yellow arrows), suggesting recalcification of the A-horizon indicated by the formation of fine sand-size micritic nodules (cyan arrows), PPL and XPL; **(D)** C3/97/PM – IIAb horizon, weakly crystallitic B-fabric in a groundmass of very fine sand-size feldspar and pyroxene grains, with the formation of a large impregnative micritic nodule (cyan arrow), suggesting recalcification of the A-horizon, PPL and XPL; **(E)** C13/98/PM – base of IIAb horizon, intermixed fabrics with undifferentiated and weakly crystallitic B-fabric and a rounded pottery fragment in the middle of the frame, suggesting some degree of land use associated to the Late Neolithic occupation of the area, PPL and XPL.

moderately high content (around 10%) of $CaCO_3$. On the contrary, the calcium carbonate of Unit 5, Area 3 is <2%. Also, the organic carbon varies between 1.5 and 3% in all samples, excluding one sample of Unit 5 where it is <0.5%. Finally, the bulk density of the archaeological units fluctuates moderately, peaking at 16% in Units 3 and 5.

4.2.2. Micromorphology

Samples for micromorphological analysis were taken from Stratigraphic Units 2, 3, 4, 4b, and 5 (Figure 7A). A summary of the micromorphological components is presented in Table 2. Most of the mineral and organic components are the same in all samples, although there are variations in the abundance of some components and of pedofeatures. Generally, the fabric of these units is random. However, sorted and very fine sand-size grains characterize most of the sediment samples. These sand grains are equant and subangular; the coarser ones are mainly composed of marl, chert, trachyte and lava fragments, with sanidine and plagioclase prevailing among the finer grains. The mineral grains are embedded in a micromass of yellow-brown (in PPL, dark brown in XPL) clayey silt, partially composed of grayish-brown ash crystals (rhomboidal pseudomorphs of calcium oxalates) and fragmented phytoliths. The B-fabric is always undifferentiated (Figure 7B), except in Unit 2 which shows a marked crystallitic B-fabric (Figure 8A). Commonly, the structure is very porous (Figure 7C), with common planes and fewer channels. All these sedimentary units are characterized by abundant organic materials. Fresh and burnt bones ranging in size from 5 mm to 0.5 mm and mollusk shell fragments are very common in all Units 2, 3, 4, 4b, and 5 (Figures 7D, 8A, D). Charcoal fragments from 1.5 to <0.5 mm, strongly humified vegetal remains, and silt- to fine-sand size amorphous organic materials are widely present in all the sampled units (Figure 7E). Further among the organic components, rounded excrements with a diameter of 1 mm are found in Units 4, 4b, and 5 (Figures 8B–E). These are composed of yellowish amorphous organic matter with few fragmented phytoliths and silt-size mineral grains, sometimes showing a convolute structure with fibrous voids. They also display fecal spherulites with the typical extinction crosses in XPL (Figure 8F). Among the inorganic components of organic origin, ash and phytoliths are the dominant constituents, followed by common pottery fragments and lithic debris. Phytoliths are numerous in all samples, particularly in Units 4, 4b, and 5, and their shapes are mostly elongate entire, with curved faceted surfaces, acute, dentate, and flabellate bulliform. In some cases, particularly in Units 4b and 5, very well-sorted fragmented phytoliths, silt, and very fine form crust-like lenses (Figures 7E, 8H). Interestingly, many Non-Pollen Palynomorphs (NPPs) are recorded in thin sections, particularly from Units 4 and 5. A cluster of spheroidal fungal spores, 10–20 μm in diameter, is present in Unit 4. Another NPP from this unit resembles an oocyst of coccidia, which are parasites that affect the intestinal tract of animals (Égüez et al., 2020). From Unit 5, a 1-mm wide sub-circular fungal sclerotium (probably *C. geophilum*) and a fungal spore composed of a closed spherical shell containing black rounded elements are found. The pedofeatures identified in the archaeological deposits are predominantly impregnations, coatings, and crystalline pedofeatures. Matrix impregnation by Fe-Mn oxides, nucleic, and concentric Fe-Mn nodules are very common in Units 3, 4, and 5, which develop around volcanic rock fragments or a former root and feature alternating bands of fine grains and amorphous Fe-Mn cement. In addition, calcitic pedofeatures are found in variable quantity in all samples of Units 2 through 5. The groundmass of Unit 2 is strongly impregnated by micritic calcite forming numerous typic nodules, as well as coatings and hypocoatings within channels (Figure 8A). On the other hand, very few micritic hypocoatings and needle-fiber calcite channel coatings are detected in Units 3, 4, 4b, and 5, which on the contrary is completely depleted of calcite in several areas. Also, orange typic and convolute nodules and amorphous impregnations of phosphatic material appear frequently in Units 4, 4b, and 5. Interestingly, at the base of Unit 5 from Area 3, dirty clay, with brown to bright yellowish-brown color in XPL, coats compound voids, mineral grains and channels. Interestingly, an aggregate composed of sand grains and dark-brown organic material is present in Unit 5, capped by very fine sand grains and organic material organized in a laminated fabric (Figure 8G). Finally, rounded blocky fragments of Vertisol peds with sharp boundaries, are randomly distributed in Units 4, 4b, and 5 (Figure 8D).

4.3. The sedimentary units from areas 19 and 20

Four soil blocks and bulk soil samples were collected from Units B, C, D, and DP, which represent the group of sedimentary units identified on the western slopes of the Contraguda hill, in Areas 19 and 20.

4.3.1. Physical-chemical parameters

Only the units from Area 20 were sampled and analyzed for $CaCo_3$ and organic C content. However, also Area 19 was sampled for bulk density, thus providing quantitative data for the units of these areas. Units B and C (samples C14, and C15) display a moderate calcium carbonate content, and their organic C is attested between 0.4 and 0.7%. The bulk density of these two units is slightly higher than those of Area 19, where units D (C24) and DP (C25) reach 5 and 11% respectively.

4.3.2. Micromorphology

A summary of the micromorphological characteristics of Units B, C, D and DP is listed in Table 2. The main distinguishing features of these sediments are presented here.

4.3.2.1. Area 20, units b and c

These two units found in Area 20 will be described together, as their components and structure are significantly similar. They are both characterized by a sandy loam texture, with a clayey silt micromass surrounding moderately to poorly sorted fine sands. Both of them also show a weakly separated sub-angular blocky structure. The organic content is considerable in both units, including prevalently hardwood charcoal fragments, fresh and burnt bones (Figure 9B), humified plant remains and amorphous

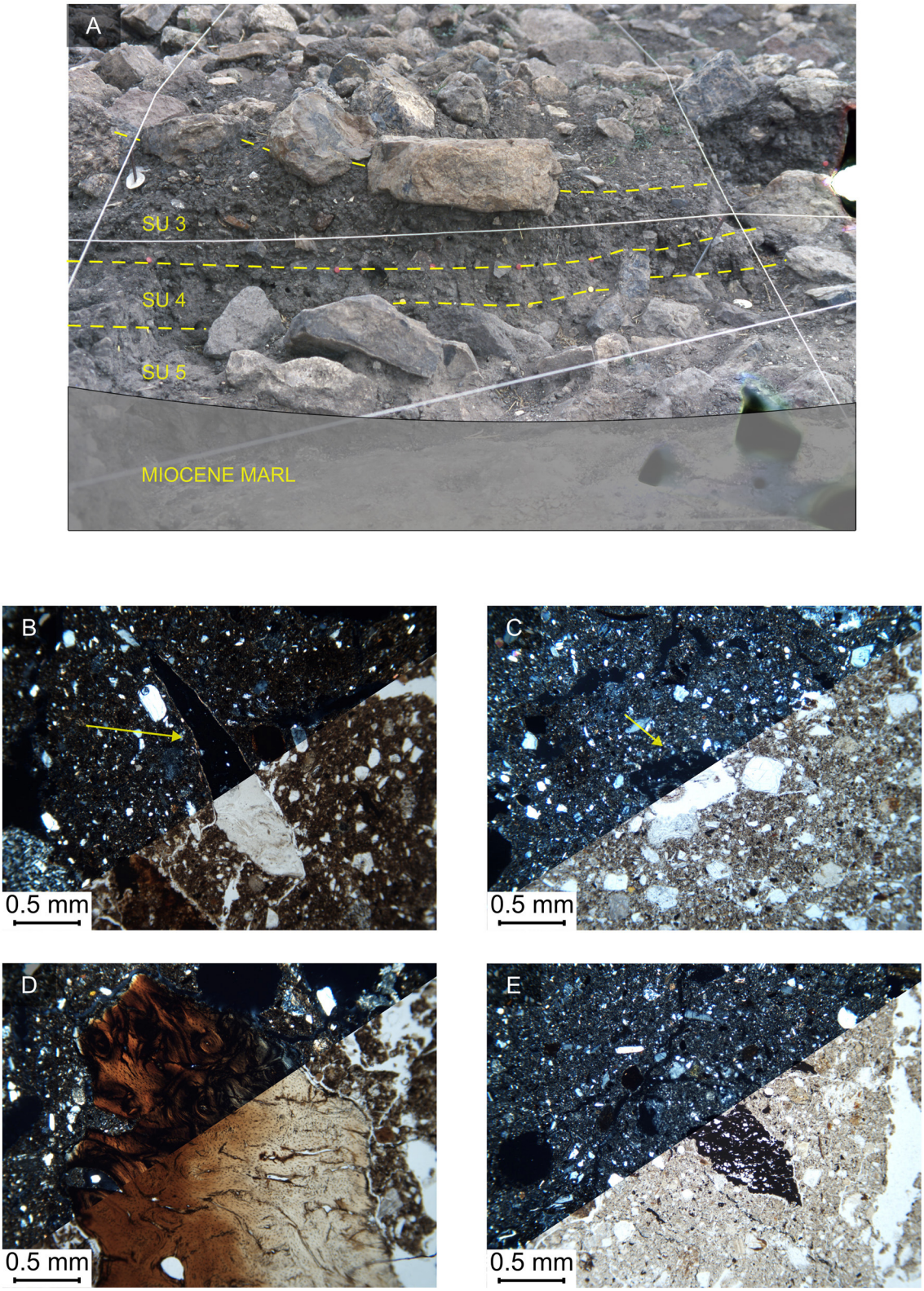

FIGURE 7
(A) Field photograph of Units 3, 4, and 5 as a fill of a pit in Area 3 that was cut into the marl bedrock; **(B)** C23/98/3 – Unit 3, humic groundmass material with very fine sand grains and artifacts. In this case, an obsidian micro flake (yellow arrow) with a very inclined orientation is an indicator of a chaotically organized sediment, PPL and XPL; **(C)** C22/98/4 – Unit 4, very fine groundmass composed of finely dispersed ash crystals and fragmented phytoliths, with a transversal section of a grass root in a channel (yellow arrow) suggesting that this deposit remained exposed and colonized by grasses, PPL and XPL; **(D)** C21/98/5 – Unit 5, large burnt bone fragment with very inclined orientation in a very fine groundmass, PPL and XPL; **(E)** C21/98/5 – Unit 5, groundmass of finely dispersed ash crystals and fragmented phytoliths, with sand-size charcoal fragments, showing a chaotic distribution, PPL and XPL.

TABLE 2 Components of the archaeological deposits of Areas 3 and 4 of Contraguda.

Component	Description and comments	Occurrence
Volcanic rock fragments	Generally subangular blocky fragments of ignimbrite and pyroclastic rocks. Granule to fine pebble size. Randomly distributed and oriented. In one case linear distribution and grading.	All; graded: C4/97/4
Marl fragments	Generally subrounded blocky fragments with dissolution weathering. Granule to fine pebble size. Randomly distributed and oriented.	Unit 2
Sand	Mainly K-feldspars and plagioclases, pyroxenes and chert in minor amounts. Also sand-size rock fragments. Randomly distributed and oriented dominantly angular to subangular.	All
Silt	Mostly feldspars and calcite.	Occurs in significant amounts in all samples.
Clay	Coarse and dirty due to amorphous organic and sesquioxide impregnations. Brown in PPL; extinct in XPL	Occurs in modest amounts in all samples.
Fine clastic elements		
Calcareous ash	Varies significantly between Units and Areas, although generally rare having been subjected to decalcification. It is mainly found scattered and mixed with the micromass	Occurs in modest amounts in all samples
Organic elements		
Bone	Generally sand to centimeter-size pieces angular to subangular Burned and fresh Chaotically distributed	All
Charcoal: wood	Sand-size pieces Angular to subangular in some cases showing the banded vessel structure of hardwood can be discerned, though the majority are non-descript pieces chaotically distributed isolated pieces. Very fine sand-size pieces occur in phytolith-rich lenses	All
Charcoal: fibrous	Medium to very fine sand-size pieces subangular blocky or platy Mostly occur as oxidized plant remains	All
Spores	10 μm – spheroidal violet occurring in clusters 50 μm – ellipsoidal brown as isolated elements 500 μm – hyphae exocarp containing circular dark purple elements 1000 μm – black hyphae exocarp containing 10 μm-wide white spheres, extinct in XPL	C4/97/4, C10/97, C12/98/5
Inorganic elements		
Mollusk shells	Medium-sand size Subangular isolated pieces	C05/97/4b, C17/98/4
Phytoliths	Mostly elongate entire also articulated as beam/bundles Elongate dentate bulliform types consists mainly of *Poaceae* grasses occur in non-laminated distribution and mixed with fine mineral grains and charcoals	All; C16/98/5 very well-sorted phytolith and charcoals with silt-size grains
Pottery fragments	Sand to centimeter-size subangular isolated pieces with reddish colors coarse and fine fabrics	C4/97/4, C5/97/4b, C10/97, C11/97/5, C12/98/5, C21/98/5, C22/98/4, C23/98/3
Lithic debris	Chert and obsidian micro flakes or debris fragments sand to centimeter-size	C4/97/4, C21/98/5, C23/98/3, C25/98/DP
Excremental elements		
Small mammal excrements	~0.5 – 1.5 mm in diameter rounded aggregates of massive brown organic matter with very fine sand grains, tiny phytolith fragments, and fecal spherulites; sometimes showing a fibrous-convolute fabric. Isotropic in XPL Isolated pieces	C4/97/4, C5/97/4b, C11/97/5, C16/98/5
Dung crust	~4 mm long the subrounded blocky aggregate of medium sand grains and brown organic material, capped by laminated fibrous organic material in a phosphatic mass. Isotropic in XPL Isolated piece	C16/98/5
Pedofeatures		
Crystallitic: calcite-related	Coarse to fine sand-size calcitic nodules, micritic hypo-quasicoatings, and groundmass impregnation from geogenic calcium carbonates (i.e., weathered marl fragments)	C9/97/2
	Micritic hypocoatings from dissolved and recrystallised calcitic ash	Units 3, 4, 4b, 5, B, C
	Needle-fiber calcite coatings of channels (*pseudo-mycelium)*	Units 3, 4, 4b, B, C; very abundant in Unit 5

(Continued)

TABLE 2 (Continued)

Component	Description and comments	Occurrence
Crystallitic: phosphate-related	Typic, septaric, and anhedral nodules of orange phosphate isolated pieces in areas with phytoliths, charcoals, and bones	C4/97/4, C19/98/3
Crystallitic: iron-manganese-related	Amorphous impregnations typic, concentric, and geoidic nodules randomly distributed	Very abundant in C17/98/, C19/98/3, C23/98/3, C20/98/5, C21/98/5
Textural: silty clay	Dirty, non-oriented, non-laminated, silty clay coating of channels and compound voids	C12/98/5, C15/98/C
Textural: pedorelicts	Sand-size fragments of soil aggregates with sharp boundaries, composed of yellow silty clay and fine sand grains, originated from vertisol materials isolated pieces	C4/97/4; C5/97/4b; C12/98/5; C14/98/B; C15/98/C; C16/98/5; C20/98/5;

organic matter. Small, 0.5 mm width, rounded excrements composed of isotropic amorphous yellowish phosphatic material are occasionally found in Unit C, together with very fine sand to silt-size mineral grains and very few fecal spherulites (Figure 9C). Among the inorganic components of organic origin, highly fragmented phytoliths are common in both Units. Bulliform, elongate entire, and more rarely spheroidal granulate are the most common types identified. Pottery fragments are also recorded in Unit B (Figure 9A). The pedofeatures identified in these sedimentary units are mainly textural. Both units include Vertisol pedorelics chaotically scattered throughout the groundmass. On the other hand, Unit B display some *in situ* clay coatings along interpedal channels; these coatings are composed of non-oriented dirty clay speckled by amorphous Fe-Mn oxides or organic matter. Finally, both samples frequently show infillings of excremental pellets within channels due to soil mesofauna activity.

4.3.2.2. Area 19, unit d

This unit is characterized by a juxtaposition of peds with different fabrics. Angular blocky peds composed of dark brown silty clay with stipple-speckled B-fabric and sandy loam texture are mixed with reworked orange-brown clay loam peds, analogous to those of Unit DP. Numerous bone fragments and coarse-sand size charcoal characterize the organic content of this unit, together with humic materials (Figure 9E). Various phytoliths are also detected through the dark brown silty clay groundmass. The elongate entire type is the most frequent, although elongate dentate, crenate, and bulliform types are also recorded. Textural pedofeatures characterize both two fabric types. *In situ* non-laminated dusty clay coatings are identified along channels at the bottom of the slide (Figure 9F). The upper part includes fragments of horizontally oriented silty clay crusts whose thickness ranges between 0.5 and 0.1 mm and that appear bioturbated by channels (Figure 9D).

4.3.2.3. Area 19, unit DP

This unit is characterized by angular blocky peds with clay loam texture, orange-brown in PPL and bright yellowish brown in XPL (Figure 9G). The B-fabric features well-expressed striations, such as random, and grano-striations (Figure 9G). The mineral fraction includes mainly plagioclase, pyroxenes, trachyte fragments of fine sand-size, and fewer coarser grains composed of volcanic rock and chert. On the other hand, a fabric much richer in humic materials is also present within the interpedal channels. Here, the organic content is more abundant than in the clay loam peds, and it is rich in bone fragments, charcoal and humic material. Among the mineral components, a 3-mm long, platy obsidian microlithic flake,

TABLE 3 Summary of the major results retrieved in this study.

Human behavior	
Geoarchaeological understanding of Middle Neolithic – *San Ciriaco* settlement patterns	Anthropogenic materials dumped in pits across the settlement area originated from household maintenance activities (sweeping house floors; raking-out hearths) and sheep/goat herding (possibly in shared living spaces)
Late Neolithic – *Ozieri* ephemeral occupation	Scarce anthropogenic materials mixed with colluvium in pits from a restricted area, indicating episodic occupation
Formation processes of site stratigraphy	
Middle Neolithic – *San Ciriaco* deposits	Slow formation of archaeological deposit indicated by rare lenses of materials, intense bioturbation throughout, and sheetflow deposits due to rainstorms; humid climate conditions as suggested by absence of pedogenic calcite and dissolution of carbonates
Late Neolithic – Ozieri deposits	Colluvial inputs as indicated by numerous marl fragments; dry climate conditions as suggested by strong micritic impregnations and pedogenic micritic nodules
Land use	
Middle Neolithic – San Ciriaco agriculture	Earliest evidence of plowed agriculture in Sardinia indicated by pedofeatures detected in the Verti-paleosol (shear-stress features in the plow zone; soil crusting; mixing of upper/lower A-B soil horizon materials; unsorted silty clay coatings) combined with soil amendment practices (high input of midden-like materials enhancing the organic content)
Human-environmental interactions	
Human-induced soil changes and landscape transformation	Transformation of a brown forest soil (Alfisol) into a grassland Vertisol after forest clearance (*in situ* dirty clay coatings capping soil peds and dislodged/fragmented laminated limpid and dusty clay coatings); desertification and deterioration of the landscape due to prolonged land use impacts and intense soil erosion.

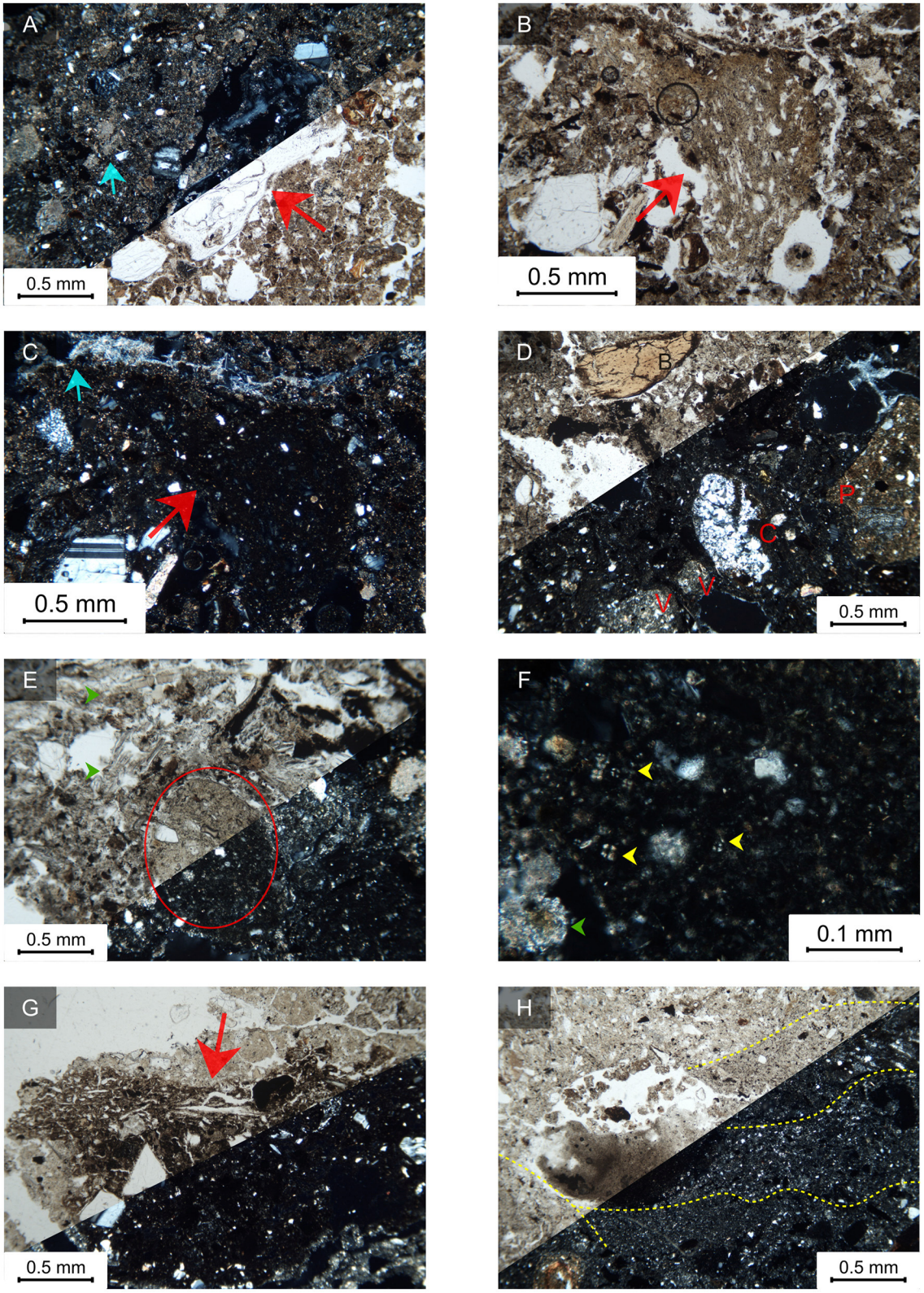

FIGURE 8
Microphotographs of Units 2, 4, 4b, and 5 from Areas 3 and 4. **(A)** C9/97/2 – Unit 2, groundmass rich in geogenic and pedogenic (blue arrow) calcite, with midden-like materials such as bone fragments (red arrow), PPL and XPL; **(B)** C5/97/4b – Unit 4b, very fine, non-calcareous, groundmass with a fragmented sheep/goat coprolite (red arrow), showing a convolute structure and rounded shape and reworked by soil fauna, suggesting that domesticated animals were kept around the settlement area; **(C)** same as B in XPL, showing the isotropic properties of the sheep/goat coprolite (red arrow) and of the micromass, also showing needle-fiber calcite channel coating (cyan arrow). The latter forms due to fungal biomineralization and decay of the organic matter inside fungal walls (Durand et al., 2018), suggesting dung-related high bacteria levels in the sediment; **(D)** C5/97/4b – *(Continued)*

FIGURE 8 (Continued)
Unit 4b, chaotically organized groundmass composed of finely dispersed ash, charcoals, and phytoliths, bone fragments (B), chert (C), rounded Vertisol fragments (V) and pottery shards (P), with needle-fiber calcite channels coatings (cyan arrow), suggesting that the unit represents a dumped deposits with early evidence of Vertisol erosion, PPL and XPL; **(E)** C11/98/5 – Unit 5, groundmass composed of finely dispersed ash crystals, phytoliths and charcoals, with areas richer in phytoliths (green arrows), and showing a rounded sheep/goat coprolite, suggesting that this sediment originated from the maintenance of spaces where domesticated animals were kept, PPL and XPL; **(F)** detail of the coprolite in D, showing fecal spherulites (yellow arrows) in an amorphous phosphatic mass with undifferentiated B-fabric; note also druses from wood ashes in the sediment groundmass, XPL; **(G)** C16/98/5 – Unit 5, a fragment of dung crust characterized by laminated fabric (red arrow) capping a mineral-rich part cemented by an amorphous isotropic, dark organic material, PPL and XPL; **(H)** C16/98/5 – Unit 5, faint bedding of very fine sand- and silt-size materials mainly composed of fragmented phytoliths, mineral grains, and charcoals, suggesting different dumping episodes of household waste, originated from raking-out of hearths and floor sweeping, PPL and XPL.

probably cut oblique to its major axis, is present in an interpedal channel (Figure 9H). The pedofeatures are typic and concentric nodules of pure Fe or Fe-Mn oxides, often cementing very fine sand grains. As noted in the soil samples from Areas 3 and 4, there are fragments of dislodged laminated dusty clay coatings scattered throughout the groundmass.

5. Discussion

The results of the micromorphological study combined with the physical-chemical analyses provided important insight into the human practices that produced the archaeological deposits of Contraguda (Table 3). Moreover, our study unraveled a sequence of major paleopedological changes that occurred during the Middle Holocene directly linked with the earliest geoarchaeological evidence of agricultural practices in Sardinia (Table 3).

5.1. Genesis of the archaeological deposits of contraguda

The results of the geoarcheological study of the sedimentary units suggest that the archeological sequences of Areas 3 (SU 2, 3, 4, 5), 4 (SU 3, 4, 4b, 5), and 20 (B and C) were originated and accumulated by human activities through a relatively long series of actions. Even if bioturbation due to meso-macro-fauna activity sometimes resulted in chaotic re-organization of the sediments, depositional processes and environments could be identified in many cases.

All units are characterized by a rather chaotic sediment composed of sand-size clasts randomly dispersed within a fine fraction of calcitic ash, phytoliths, and humic materials, with complex porosity composed mostly of bioturbation channels and complex packing voids. All these features belong to the typical microstructure of dumped midden-like sediments (Matthews et al., 1997; Shillito et al., 2011; Shillito and Matthews, 2013; Gutiérrez-Rodríguez et al., 2018; Karkanas and Goldberg, 2019; Portillo et al., 2019). The lack of re-organization and horizontal displacement of components also suggests that these sediments did not incur further trampling after the deposition (Miller et al., 2010).

On the other hand, some micromorphological features provide insight into the cyclicity and frequency of ancient waste dumping activities at Contraguda. Among these features, Unit 4 from Area 4 includes a small lens of fine gravel grading to coarse sand, suggesting that the underlying anthropogenic deposit remained exposed after dumping and that some geogenic material was subsequently deposited over it, most likely by sheet-wash processes possibly due to thunderstorms (Karkanas and Goldberg, 2019). Moreover, samples from Unit 5 display indicators of crusting, which originated when the deposit remained exposed for some time before the next dumping episode. Increasing evidence suggests that long exposure of the dumped materials and low discarding frequency can be inferred from occasional lenses with different texture and a significant degree of bioturbation, testified by root and faunal channels (Matthews et al., 1997; Shillito and Matthews, 2013; Gutiérrez-Rodríguez et al., 2018; Portillo et al., 2019). In addition, as reported in other contexts (Wieder and Yaalon, 1982; Gutiérrez-Rodríguez et al., 2018), calcite hypocoatings associated with root growth, and by extension calcite dissolution features, are indicative of long-term exposure.

However, it can be observed that the fabric of Unit 2 clearly differs from the rest of the other archaeological units. It is much richer in marl fragments and pedogenic carbonates – mostly micrite nodules – that are larger than in the other units, and the groundmass is diffusely and strongly impregnated with micrite. This unit also lacks needle fiber calcite coatings and the typical midden-like materials such as phytoliths and ashes, and generally, the sediment looks coarser. These indicators suggest that climate conditions at Contraguda were significantly drier during the Late Neolithic, with strong development of pedogenic calcite features in the groundmass of Unit 2. Furthermore, its fabric differs significantly from the other units, likely indicating a less important or a different type of occupation of the Contraguda hill, possibly reflecting episodic activities without stable settlement.

The composition of the Middle Neolithic units located in Areas 3, 4, and 19, suggests that these likely represent waste produced by domestic activities such as cooking, maintenance of household spaces, and sweeping and raking out of hearths, which was eventually dumped inside the pits. Phytoliths, ash, charcoal, pottery fragments, and lithic artifacts are all proxies of anthropogenic sediments produced in domestic structures that were likely present in the surrounding, and that were eventually dumped into pre-existing pit features and/or onto the surface.

Additionally, excrements of herbivores were identified in Units 4, 4b, and 5, thus supporting the hypothesis based on the archeozoological findings that domestic animals, mainly sheep/goats, were herded at Contraguda (Boschian, 2003). Herbivore excrements were found dispersed in the archaeological deposits, not organized in lenses or related to other components of the sediment. Small, rounded aggregates with compact structure, brownish rims due to oxidation and humification, and in one case also the typical convolute internal structure can be fragmented sheep/goat droppings, since they also include fecal spherulites

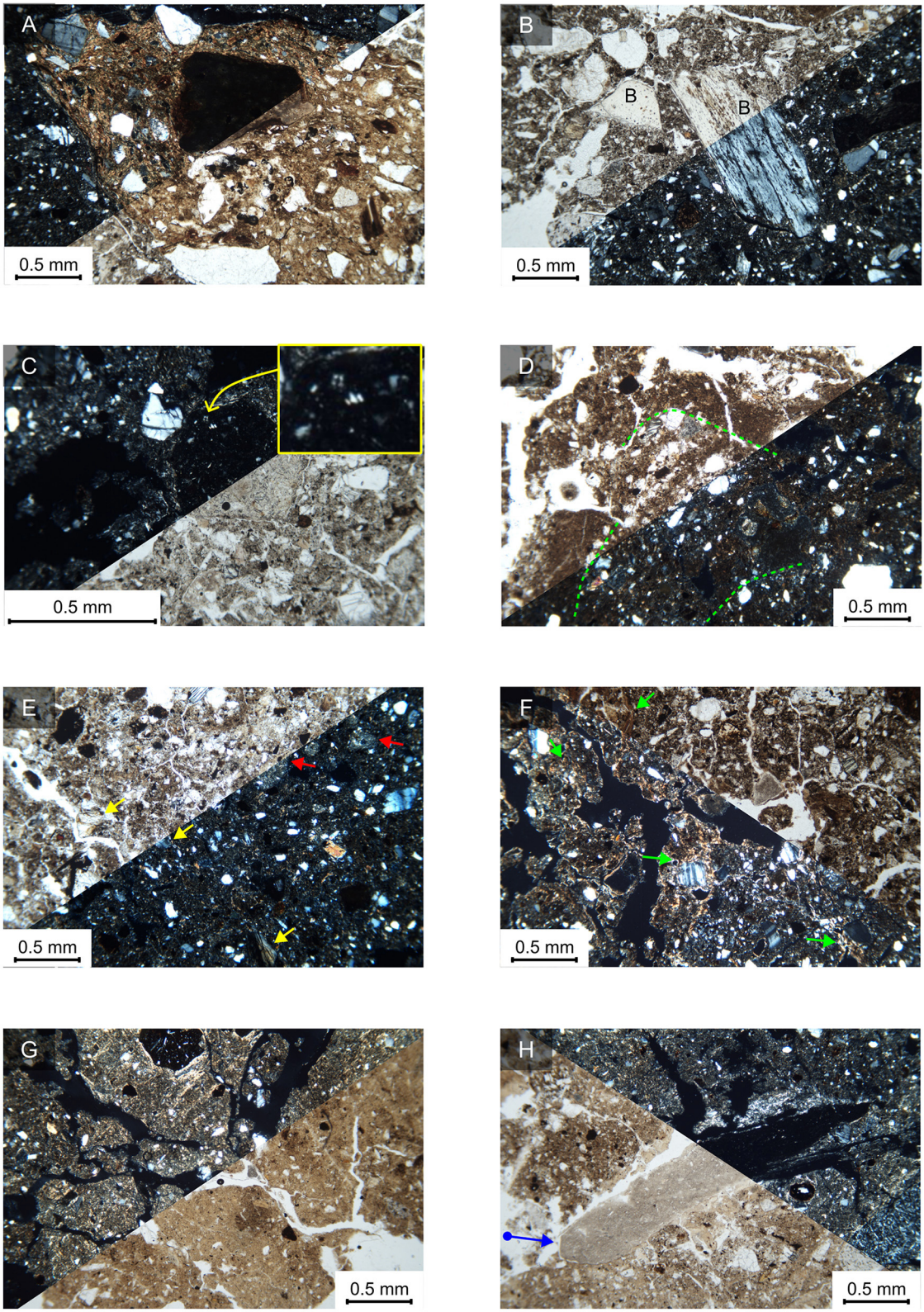

FIGURE 9
Microphotographs of the sedimentary units from Areas 19 and 20. **(A)** C14/98/B – Unit B, Area 20, pottery fragment in a groundmass of finely dispersed phytolith fragments and organic materials, XPL; **(B)** C14/98/B – Unit B, Area 20, burnt bone fragments randomly dispersed in a groundmass rich in organic materials and phytoliths. This composition suggests that the sediment originated from household maintenance activities similar to those of Areas 3 and 4, PPL and XPL; **(C)** C15/98/C – Unit C, Area 20, rounded coprolite composed of amorphous brownish organic material, isotropic, also showing few fecal spherulites of ca. 20 μm (inset), possibly originated from sheep/goat droppings, indicating animal husbandry

(Continued)

FIGURE 9 (Continued)
activities occurring in this area; **(D)** C24/98/D, Unit D, Area 19, fragments of silty clay crusts at the top of Unit D. They form due to the impact of raindrops on bare plowed soil surfaces (Courty et al., 1989; Williams et al., 2018), therefore Unit D can be regarded as a buried Ap horizon, PPL and XPL; **(E)** C24/98/D, Unit D, Area 19, groundmass of the buried Ap horizon characterized by humic silty clay, bone fragments (yellow arrows), and fragments of a Bw-horizon (red arrows), linked to mechanical mixing after plowing and soil amendment activities, PPL and XPL; **(F)** C24/98/D, Unit D, Area 19, basal part of the buried Ap horizon, characterized by chaotic dusty clay coatings mixed fine and very fine sand grains (green arrows). These textural pedofeatures are also called agricutans and occur at the base of plowed soil horizons (Jongerius, 1970; Courty et al., 1989), PPl and XPL; **(G)** C25/98/DP, Unit DP, Area 19, angular sandy clay loam peds with random and grano-striations, suggesting this is buried Bw horizon of a Vertisol, whose A-horizon has been modified and transformed into the overlying plowed Ap-horizon, PPL and XPL; **(H)** C25/98/DP, Unit DP, Area 19, an obsidian micro flake (blue arrow pointing to the flake butt), cut along its longitudinal axis, mixed with dirtier humic materials among sandy clay loam peds. This artifact, probably a by-product of obsidian agricultural tools, could have been incorporated at depth as surface material falling into desiccation cracks, PPL and XPL.

(Karkanas, 2006; Brönnimann et al., 2017). Moreover, an isolated element from Unit 5 of Area 3 showing a laminated fabric strongly resembles a fragment of stabling crust, which derives from the horizontal alignment of mineral grains and vegetal constituents due to trampling by penned flocks (Brönnimann et al., 2017; Shahack-Gross, 2017).

No conclusive evidence of residential structures was found during the archaeological excavations. Only recently, rectangular structures – ascribed to the Late Neolithic-Early/Mid Copper Age according to the lithic and ceramic assemblages – were identified not far from Contraguda (Robin et al., 2022), and are the only examples of Neolithic houses discovered in the region so far. Significantly, the dumping of domestic waste into pits nearby the residential areas appears to be a common practice among the Middle Neolithic-B communities, as it was documented at the site of Su Mulinu Mannu dated to the same time interval of Contraguda (Ucchesu et al., 2017), and among other Mediterranean settlements such as that of Neolithic Çatalhöyük (Portillo et al., 2019) or Catignano in Central Italy (Boschian and Colombo, 2009). However, it is interesting to note that domestic waste and herbivore excrements were found in the midden-like deposits without distinct distribution but intermixed in similar proportions with domestic waste. This would also explain the high number of coprophilous fungi spores and intestinal parasites found throughout the groundmass of the archaeological deposits. It might be the case that domesticated animals were kept very close to the house spaces (Kvavadze et al., 2019) if not in the same areas, so that animal penning refusal and household waste were accumulated and dumped together during sweeping and maintenance activities. This behavior reminds us of the cave sites simultaneously occupied by flocks and shepherds (Brochier, 1983; Boschian, 1998; Boschian and Montagnari-Kokelj, 2000), although the proper depositional facies of these environments (Angelucci et al., 2009) was not found at Contraguda.

5.2. Evidence of anthropogenic soil changes in the middle holocene

The results of the micromorphological and physical-chemical study carried out on the buried soils of Areas 3 and 4 at Contraguda demonstrate that marked pedological changes occurred in northern Sardinia during the Middle Holocene (Figure 10). In addition, while differing completely from the archaeological deposits, the characteristics of units D and DP from Area 20 indicate that these two units are surface and subsurface horizons respectively of the same Vertisol of Area 4.

The superimposed textural pedofeatures that were found from the bottom to top horizons of the Vertisol, provide a fundamental insight into the genesis and history of this soil. The occurrence of Terra Rossa-like pedorelics indicates that a Pleistocene Terra Soil (probably an Alfisol) formerly existed on the Contraguda hill, possibly formed on older river terrace deposits (Boschian, 2003). Fragments of clay coatings, pure and fine dusty, laminated, can be commonly detected, dislodged from their original illuvial sites, in the B-horizon of the buried Vertisol. Clay coatings are unusual in Vertisols, particularly those with fine laminated fabric; and where they have been documented, they feature a deformed kink-band fabric (Stoops, 2003; Kovda and Mermut, 2018). Instead, these pedofeatures can be considered here as relics of former brown forest soils, since laminated illuvial clay coatings form in soils under dense forest cover and moist subhumid climates, where water percolation is slowed down by the closed canopy, and allows low energy settling of translocated clay (Fedoroff and Goldberg, 1982; Bullock and Thompson, 1985; Gebhardt, 1993; French, 2005; Kühn et al., 2018). Moreover, broadleaf deciduous or evergreen tree taxa are not associated with vertic soils, because the shrinking and swelling pedoturbation damages their rooting system (Ahmad, 1983; Buol, 2011). In addition, relic properties of brown forest soil might have been preserved not only in the pedofeatures found in the buried Vertisol but also in their physical-chemical properties. The organic carbon content clearly shows a vertical distribution that still reflects the pattern of Alfisol or Inceptisol horizons, which are characterized by a pseudo-exponential decrease from the A- to the base of the B-horizon. On the contrary, it has been documented that the organic content of Vertisols is nearly constant throughout their thickness, because of the pedoturbation process of self-mulching due to shrinking-and-swelling (Becker-Heidmann et al., 2002; Kovda et al., 2010). Therefore, we may infer that a well-developed brown forest soil (Alfisol or Inceptisol) associated with a dense vegetation cover existed at Contraguda during the Early and Middle Holocene, until the first Neolithic settlement of the hill. In the Mediterranean region, the formation of illuvial horizons has been linked to past moister climate conditions, such as those of the Pleistocene or Early Holocene (Fedoroff, 1997; Yaalon, 1997). However, the dense canopy of evergreen broadleaf oak forests and their thick *mull* A-horizon can create and keep moist pedoclimatic conditions even in dry atmospheric conditions such as those of the Mediterranean region (Eyre, 1963).

Observing the fossil pollen sequences retrieved on the island so far, *Erica spp.* shrubland taxa were dominant in the arboreal pollen record until 5500 cal BP (Beffa et al., 2016; Melis et al., 2018; Pedrotta et al., 2021). Around 5500 cal BP, a much less pronounced seasonality in the West Mediterranean favored the expansion of evergreen holm oak forests in Sardinia at the expense of the drought-tolerant *Erica spp.* (Beffa et al., 2016; Pedrotta et al., 2021). On the other hand, our study suggests that a dense vegetation cover, possibly composed of a holm oak forest mixed with other evergreen taxa, such as *Arbutus unedo*, *Erica arborea*, and *Phyllirea latifolia*, as is often the case in the island (Vacca et al., 2018), extended on the Contraguda landscape until 6300 years cal BP. Significantly, brown forest soils with mull-like surface horizons, are considered the climax soil association of holm oak forest formations in Sardinia (Vacca et al., 2018). When the Contraguda hill was settled by the Middle Neolithic – *San Ciriaco* communities, forest clearance and land use caused permanent disruptions in the Early/Middle Holocene soil-vegetation ecosystem. Interestingly, a decline of *Q. ilex* and *Erica spp.* is recorded between 6500 and 6100 cal BP in the north-western Sardinia fossil sequence of Lake Baratz, concurrently with a major peak in the dung fungal spores *Sporormiella* and an increase in indicators of pastoral activity and cereal farming (Pedrotta et al., 2021).

Following the impact of land use caused by the Middle Neolithic – *San Ciriaco* settlers, a new human-induced soil-forming cycle started on the Contraguda hill with the development of a grassland Vertisol. Significantly, Vertisol formation has been documented after the erosion of surface A-horizons, due to the loss of a former vegetational cover, which exposes the argillic horizon to cracking and triggers vertic processes (Buol, 2011, and references therein). Direct evidence of forest clearance is recorded in the textural pedofeatures of the Contraguda Vertisol. Prehistoric wood clearance activities, such as slash-and-burn and up-rooting, have frequently been suggested by clay coatings rich in fine charcoal, also microlaminated, formed in soils and paleosols of the European region (e.g., Macphail et al., 1990; French, 2005, 2022; Lewis, 2012; Macphail and Goldberg, 2018). Similarly, traces of clearance activities at Contraguda are recorded by *in situ* microlaminated dirty clay coatings rich in microcharcoal. These are superimposed to laminated limpid clay coatings, and also coat channels, or cap soil peds and bone fragments throughout the mid and lower part of the Vertisol.

After the vertic processes were set off on the former well-developed brown forest soil, the Middle Neolithic – *San Ciriaco* communities started extensive land-use activities on the newly formed Vertisol between 6300 and 6000 cal BP. Strikingly, this soil is characterized by features often observed in thin sections of buried soils and experimental fields, which typically form after plowing or tillage (e.g., Lewis, 2012; Deák et al., 2017). One of the most significant features recorded in the upper part of the buried A-horizon of Area 19 (C24-D) are fragmented silty-clay crusts. The formation of these crusts has been widely documented on bare arable topsoil and is due to rain splash erosion (Courty et al., 1989; Goldberg and Macphail, 2006; Williams et al., 2018). In Area 4, a compaction zone with shear stress-related features lies along the abrupt wavy boundary between the humic A-horizon and the underlying B-horizon. It is well known that the wavy shape of the boundary and the occurrence of shear stress features, often associated with the breaking up of textural pedofeatures, are regarded as indicators of a plow-ard zone in buried soils (French, 2005, 2022; Lewis, 2012). In addition, zones with irregularly juxtaposed peds with different characteristics resembling the A- and B-horizons are also commonly observed in the upper part of the Vertisol at Contraguda. The occurrence of mixed surface and sub-surface peds in the top part of soils has often been linked to mechanical mixing in the arable zone (French, 2022). Lastly, non-laminated dusty or dirty clay coatings mixed with mineral and organic components occur at the base of the A-horizon. Commonly called "agricutans" (Jongerius, 1970), these textural pedofeatures were recognized in modern and paleo-plowed soils (Jongerius, 1970; French, 2005, 2022; Lewis, 2012; Macphail and Goldberg, 2018), where they form when soil aggregates lying on bare arable topsoil are disrupted by impacting raindrops or by overland flow, and their residue is translocated downwards by water percolation (Deák et al., 2017).

The occurrence of only one of these features can hardly be used as evidence of prehistoric plowing (Deák et al., 2017; French, 2022). However, the association of an exceptional number and different types of agriculture-related pedofeatures in the buried vertisol of Contraguda demonstrates that plowing and other agricultural practices were carried out extensively in Sardinia by the Middle Neolithic-B communities. Significantly, cultivated cereal grains, such as *Hordeum vulgare* and *Triticum aestivum/durum*, were detected in another Middle Neolithic – *San Ciriaco* settlement dated between 6000 and 6500 cal BP on the central-western coast of Sardinia (Ucchesu et al., 2017). Furthermore, the palaeo-Vertisol of Contraguda includes an important component of midden-like materials, mainly fresh and burned bone fragments and charcoals. It is not unlikely that these were introduced into the soil aside other materials purposely added to increase fertility and stability, following the impact of agricultural practices. In Areas 19 and 4 there is evidence that these components entered the soil profile and were translocated into the subsurface horizons by shrinking-and-swelling.

The humic groundmass of the less developed buried Entisol of Area 3 includes silicate sand grains similar to those of the Vertisol, even if it formed on marly parent material. Humic peds without $CaCO_3$, separated by complex voids, are irregularly juxtaposed to carbonate-rich areas and mixed with frequent pottery shards and bone fragments. It consequently looks likely that this Entisol formed on thin colluvial deposits originating from the erosion of the well-developed Vertisol, after prolonged and intense land exploitation. The significant content of geogenic and pedogenic carbonates in this soil may have resulted from Late Neolithic agricultural practices carried out directly on the nearby weathered marl bedrock of Area 3, where thorough soil loss caused extensive denudation of this part of the hill during the Middle Neolithic phase. It seems reasonable that intense secondary calcium precipitation occurred in the Entisol profile of Area 3 during the Late Neolithic occupation phase, as also the archaeological sedimentary unit dated to this period was characterized by significantly more frequent carbonate features. This paleopedological and micromorphological evidence suggests that the climate of the period between 6000 and 5700 cal BP was much more aridic than the previous occupation phase. It is also likely that the Middle Neolithic wood clearance and

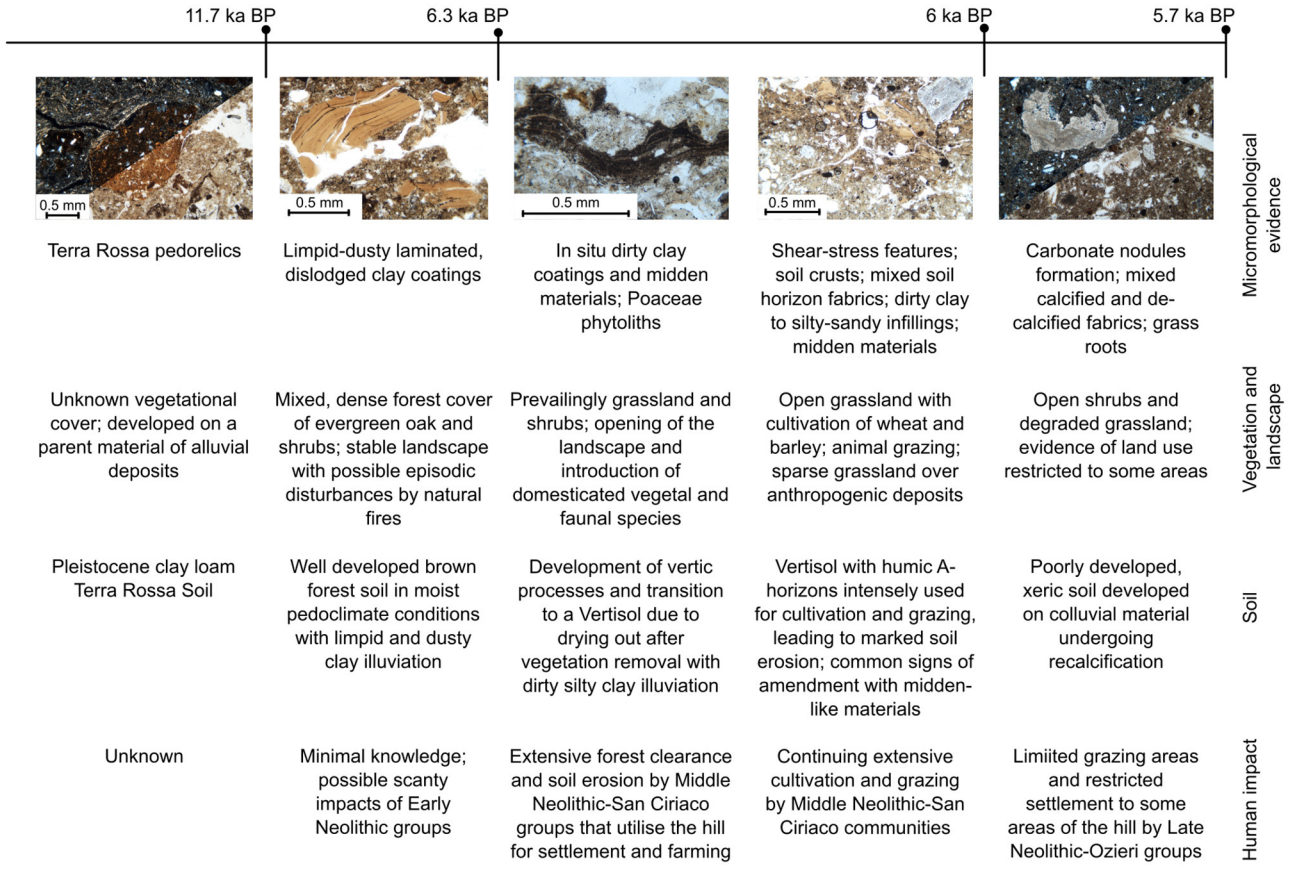

FIGURE 10
Key episodes of landscape change and human impact during the Holocene at the Contraguda hill in northern Sardinia.

intense land use led to strong desertification of the landscape, but it is also possible that the shift toward arid climate may have caused enhanced evapotranspiration rates around 6000 cal BP. As indicated by the physical-chemical analyses, this intense drying would also have caused a loss in the organic carbon within the upper horizon, because soil organic carbon dynamics in the Mediterranean region are crucially sensitive to aridification (Dvoráčková et al., 2020). In conclusion, the interplay of soil moisture loss following forest clearance, overuse and intense soil degradation linked to agropastoral and settlement activities started by the Middle Neolithic-B farmers, and a climate change toward drier conditions at 6000 cal BP may have diverted or stopped the development of the soils at Contraguda. Interestingly, these landscape processes are strikingly synchronous with those observed in the other Mediterranean island of Gozo. In that island, the impact of the temple-building Neolithic communities around 6000 cal BP disrupted the well-developed brown soils formed under a dense forest of mixed scrubland and woodland taxa and transformed them into the presently ubiquitous thin red xeric soils (French et al., 2018). The Middle Neolithic communities of Sardinia, such as those in the Maltese islands, may have had a similarly dramatic impact on the landscape history of the region through their economic and settlement lifestyle, suggesting that anthropogenic processes of land degradation started already about 6300 years ago. These environmental changes were irreversible, and continuous grazing and land abandonment in the following centuries likely prevented any soil to mature, leading to the extensive thin, xeric, Entisol covers found in the present landscape of many marly and limestone hills of northern Sardinia (Figure 11).

6. Conclusion

In contrast to the diversity of soils found buried beneath the archaeological deposits and the modern topsoil at Contraguda, the present-day pedological cover of marl hilltops across the island of Sardinia is dominated by thin weakly developed soils and denuded areas. Similarly to what was noted in other Mediterranean islands (French et al., 2018), the results of the present and previous research at Contraguda show that the current soil distribution pattern does not reflect past landscape conditions. Our geoarchaeological study of the buried soils of Contraguda highlighted a complex history of soil-human interactions occurring in the Middle Holocene when the Middle Neolithic – *San Ciriaco* communities settled in the area. Before 6300 years cal BP the Contraguda hill was host to a brown forest soil associated with a dense vegetation cover and a moister pedoclimatic regime. However, Middle Neolithic – *San Ciriaco* communities caused soil moisture loss through wood clearance. Becoming more susceptible to summer drying, the pre-existing brown

FIGURE 11
Degraded xeric grassland of *Lollium multiflorum* with *Euphorbiacae* and *Astaracae* on the Contraguda hill, delimited by a retaining stone wall. In the background land parcels with fallow crops and open-sparse shrubs under intense grazing (Boschian, 1998).

forest soil started to develop vertic processes under increasing xeric pedoclimate conditions. Extensive agricultural practices, coupled with other settlement-related activities, led to irreversible pedological and environmental changes, eventually culminating in the erosion of wide areas of the hill and the formation of a xeric carbonate-rich soil. If the renowned Sardinian archaeologist Lilliu (2004) once linked the Middle Neolithic – *San Ciriaco* pottery style to that of the *Red Skorba* cultural aspect from Malta, we can today trace a striking geoarchaeological parallel between the impact of Neolithic societies on landscape and soilscapes of these two Mediterranean islands around 6300–6000 cal BP, suggesting to re-think the timing and extent of prehistoric human impact on the paleoenvironmental history of many parts of the Mediterranean region.

Data availability statement

The original contributions presented in the study are included in the article/Supplementary material, further inquiries can be directed to the corresponding author.

Author contributions

GM: conceptualized, designed the study, performed the soil micromorphological analysis, prepared the graphics, microphotographs, and wrote the original draft. GB: carried out the geoarchaeological fieldwork, collected the samples, provided the thin sections, performed the physical-chemical analyses, and took the field photographs. All authors contributed to manuscript revision, read, and approved the submitted version.

Funding

The authors would like to acknowledge the University of Cambridge Central Open Access Funding for providing financial support to pay the open access fees.

Conflict of interest

The authors declare that the research was conducted in the absence of any commercial or financial relationships that could be construed as a potential conflict of interest.

Publisher's note

Supplementary material

The Supplementary Material for this article can be found online at: https://www.frontiersin.org/articles/10.3389/fearc.2023.1206750/full#supplementary-material

SUPPLEMENTARY TABLE S1
Full micromorphological description of the thin sections (.xlsx).

SUPPLEMENTARY APPENDIX S2
Scan of each thin section with a simplified interpreted sketch accompanied by an interpretative legend (.pdf).

References

Ahmad, N. (1983). "Vertisols" in *Pedogenesis and Soil Taxonomy. II. The Soil Orders*, eds. L. P. Wilding, N. E. Smeck, G. F. Hall (Amsterdam: Elsevier), 91–123.

Angelucci, D. E., Boschian, G., Fontanals, M., Pedrotti, A., and Vergès, J. M. (2009). Shepherds and karst: the use of caves and rock-shelters in the Mediterranean region during the Neolithic. *World Archaeol.* 41, 191–214. doi: 10.1080/00438240902843659

Aru, A., Baldaccini, P., Vacca, A., Delogu, G., Dessena, M. A., Madrau, S., et al. (1991). *Nota Illustrativa Alla Carta Dei Suoli Della Sardegna*. Cagliari: Cagliari Publishing.

Barker, G. (1995). *Mediterranean Valley*. London: Bloomsbury Publishing.

Becker-Heidmann, P., Andresen, O., Kalmar, D., Scharpenseel, H.-., W., and Yaalon, D. H. (2002). Carbon dynamics in vertisols as revealed by high-resolution sampling. *Radiocarbon* 44, 63–73. doi: 10.1017/S0033822200064687

Beffa, G., Pedrotta, T., Colombaroli, D., Henne, P. D., van Leeuwen, J. F. N., Süsstrunk, P., et al. (2016). Vegetation and fire history of coastal north-eastern Sardinia (Italy) under changing Holocene climates and land use. *Veget Hist. Archaeobot.* 25, 271–289. doi: 10.1007/s00334-015-0548-5

Binder, D., Gratuze, B., and Vaquer, J. (2012). La circulation de l'obsidienne dans le Sud de la France au Neolithique. *Rubricatum* 5, 189–199.

Boschian, G. (1998). Sedimentology and soil micromorphology of the late Pleistocene and early Holocene deposits of Grotta dell'Edera (Trieste Karst, NE Italy). *Geoarchaeology* 12, 227–249. doi: 10.1002/(SICI)1520-6548(199705)12:3<227::AID-GEA3>3.0.CO;2-4

Boschian, G. (2003). "Late Neolithic farmers and soilscape in Northern Sardinia (Italy)," in *First International Conference on Soils and Archaeology,* eds. G. Füleky (Oxford: British Archaeological Reports International Series), 29–35.

Boschian, G., Brilli, P., Falchi, P., Fenu, P., Martini, F., Pitzalis, G., et al. (2001). Prime ricerche nell'abitato neolitico di Contraguda (Perfugas, Sassari). *Rivista di Scienze Preistoriche* 10, 235–287.

Boschian, G., and Colombo, M. (2009). "Infilling processes of large pit features at Catignano – Neolithic (Italy)", in *Defining a Methodological Approach to Interpret Structural Evidence*, ed. F. Cavulli (Oxford: British Archaeological Reports International Series), 43–50.

Boschian, G., and Montagnari-Kokelj, E. (2000). Prehistoric shepherds and caves in the Trieste Karst (Northeastern Italy). *Geoarchaeology* 15, 331–371. doi: 10.1002/(SICI)1520-6548(200004)15:4<331::AID-GEA3>3.0.CO;2-H

Brochier, J. E. (1983). Bergeries et Feux de Bois Néolitiques dans le Midi de la France. *Quartär* 34, 181–193.

Brönnimann, D., and Pümpin, C., Ismail-Meyer, K., Rentzel, P., Égüez, N. (2017). "Excrements of omnivores and carnivores", in *Archaeological Soil and Sediment Micromorphology*, eds. C. Nicosia, G. Stoops (London: Wiley Blackwell), 67–81.

Bullock, P., Fedoroff, N., Jongerius, A., Stoops, G., and Tursina, T. (1985). *Handbook for Soil Thin Section Description*. Wayne, VI: Wayne Research.

Bullock, P., and Thompson, M. L. (1985). "Micromorphology of alfisols", in *Soil Micromorphology and Soil Classification*, eds L. A., Douglas and M. L. Thompson (Madison: Soil Science Society of America), 17–47.

Buol, S. W. (2011). *Soil Genesis and Classification, 6th Edn.* London: Wiley-Blackwell.

Butzer, K. W. (2005). Environmental history in the Mediterranean world: cross-disciplinary investigation of cause-and-effect for degradation and soil erosion. *J. Archaeol. Sci.* 32, 1773–1800. doi: 10.1016/j.jas.2005.06.001

Carboni, S., Palomba, M., Vacca, A., and Carboni, G. (2006). Paleosols provide sedimentation, relative age, and climatic information about the alluvial fan of the River Tirso (Central-Western Sardinia, Italy). *Q. Int.* 156, 79–96. doi: 10.1016/j.quaint.2006.05.005

Catt, J. A. (1991). Paleopedology manual. *Q. Int.* 6, 1–95. doi: 10.1016/1040-6182(90)90002-L

Courty, M. A., Goldberg, P., and Macphail, R. (1989). *Soils and Micromorphology in Archaeology*. Cambridge: Cambridge University Press.

Deák, J., Gebhardt, A., Lewis, H., Usai, M. R., and Lee, H. (2017). "Soils disturbed by vegetation clearance and tillage," in *Archaeological Soil and Sediment Micromorphology*, eds. C. Nicosia, G. Stoops (London: Wiley Blackwell), 231–264.

Di Rita, D., Ghilardi, F., Fagel, M., Vacchi, N., Warichet, M., Delanghe, F., et al. (2022). Natural and anthropogenic dynamics of the coastal environment in northwestern Corsica (western Mediterranean) over the past six millennia. *Q. Sci. Rev.* 278, 107372. doi: 10.1016/j.quascirev.2022.107372

Di Rita, D., and Melis, F. R. T. (2013). The cultural landscape near the ancient city of Tharros (central West Sardinia): vegetation changes and human impact. *J. Archaeol. Sci.* 40, 4271–4282. doi: 10.1016/j.jas.2013.06.027

Durand, N., Monger, H. C., Canti, M. G., and Verrecchia, E. P. (2018). "Calcium Carbonate Features," in *Interpretation of Micromorphological Features of Soils and Regoliths*, eds. G. Stoops, V. Marcelino, F. Mees (New York, NY: Elsevier), 205–258.

Dvoráčková, H., and Hladk,ý, J., Huesco-Gonzàlez, P., Vlček, V. (2020). Effect of different soil amendments on soil buffering capacity. *PLoS ONE* 17, e0263456. doi: 10.1371/journal.pone.0263456

Égüez, N., Dal Corso, M., Wieckowska-Lüth, M., Delpino, C., and Tarantini, M., Biagetti, S., et al. (2020). A pilot geo-ethnoarchaeological study of dung deposits from pastoral rock shelters in the Monti Sibillini (central Italy). *Archaeol. Anthropol. Sci.* 12, 114. doi: 10.1007/s12520-020-01076-4

Eyre, S. R. (1963). *Vegetation and Soils: A World Picture*. London: Arnold.

Falchi, P., Fenu, P., Martini, F., Pitzalis, G., and Sarti, L. (2012). "L'insediamento neolitico di Contraguda, Perfugas Sassari: aggiornamento delle ricerche", in *Atti della XLIV Riunione Scientifica dell'Istituto Italiano di Preistoria e Protostoria La Preistoria e la Protostoria Della Sardegna, Cagliari, Barumini, Sassari 23-28 novembre 2009, Volume II e Comunicazioni*, eds. C. Lugliè (Firenze: Istituto Italiano di Preistoria e Protostoria), 503–508.

Fanti, L., Drieu, L., Mazuy, A., Blasco, T., Lugliè, C., Regert, M., et al. (2018). The role of pottery in Middle Neolithic societies of western Mediterranean (Sardinia, Italy, 4500-4000 cal BC) revealed through an integrated morphometric, use-wear, biomolecular and isotopic approach. *J. Archaeol. Sci.* 93, 110–128. doi: 10.1016/j.jas.2018.03.005

Fedoroff, N. (1997). Clay illuviation in Red Mediterranean soils. *Catena* 28, 171–189. doi: 10.1016/S0341-8162(96)00036-7

Fedoroff, N., Courty, M. A., and Thompson, M. L. (1990). Micromorphological Evidence of Paleoenvironmental Change in Pleistocene and Holocene Paleosols. *De. Soil Sci.* 19, 653–665. doi: 10.1016/S0166-2481(08)70382-9

Fedoroff, N., and Goldberg, P. (1982). Comparative micromorphology of two late Pleistocene paleosols (in the Paris basin). *Catena.* 9, 227–232 doi: 10.1016/0341-8162(82)90003-0

French, C. (2005). *Geoarchaeology in Action: Studies in Soil Micromorphology and Landscape Evolution*. London: Routledge.

French, C. (2022). *Human Transformations of the Earth.* Oxbow, Oxford.

French, C., Sulas, F., and Madella, M. (2009). New geoarchaeological investigations of the valley systems in the Aksum area of northern Ethiopia. *Catena* 78, 218–233. doi: 10.1016/j.catena.2009.02.010

French, C., Sulas, F., Melis, R. T., Di Rita, F., Montis, F., Taylor, F. G. et al. (2016). "Evoluzione Del Paesaggio E Insediamento Nel Bacino Del Rio Posada: Indagini Geoarcheologiche", in *Sa massaria: ecologia storica dei sistemi di lavoro contadino in Sardegna: Tomo I-II*, eds. G. Serreli, R.T. Melis, C. French, and F. Sulas (Caglari: Consiglio Nazionale delle Ricerche).

French, C., Taylor, S., McLaughlin, R., Cresswell, A., Kinnaird, T., Sanderson, D., et al. (2018). A Neolithic palaeo-catena for the Xaghra Upper Coralline Limestone plateau of Gozo, Malta, and its implications for past soil development and land use. *Catena* 171, 337–358. doi: 10.1016/j.catena.2018.07.039

Gebhardt, A. (1993). Micromorphological evidence of soil deterioration since the mid-Holocene at archaeological sites in Brittany, France. *The Holocene* 3, 333–341. doi: 10.1177/095968369300300405

Goldberg, P., and Macphail, R. (2006). *Practical and Theoretical Geoarchaeology, 1st Edn*. New York, NY: Wiley.

Goldberg, P., Miller, C. E., Schiegl, S., Ligouis, B., Berna, F., Conard, N. J., et al. (2009). Bedding, hearths, and site maintenance in the Middle Stone Age of Sibudu Cave, KwaZulu-Natal, South Africa. *Archaeol Anthropol Sci* 1, 95–122. doi: 10.1007/s12520-009-0008-1

Gutiérrez-Rodríguez, M., Brassous, L., Guti?rrez, O. R., Peinado, F. J. M., Orfila, M., et al. (2018). Site formation processes and urban transformations during Late Antiquity from a high-resolution geoarchaeological perspective: Baelo Claudia, Spain. *Geoarchaeology*. 35, 258–286. doi: 10.1002/gea.21769

Jongerius, A. (1970). Some morphological aspects of regrouping phenomena in Dutch soils. *Geoderma* 4, 311–331. doi: 10.1016/0016-7061(70)90008-X

Karkanas, P. (2006). Late Neolithic household activities in marginal areas: the micromorphological evidence from the Kouveleiki caves, Peloponnese, Greece. *Journal of Archaeological Science* 33, 1628–1641. doi: 10.1016/j.jas.2006.02.017

Karkanas, P., and Goldberg, P. (2019). *Reconstructing Archaeological Sites: Understanding the Geoarchaeological Matrix*. London: John Wiley and Sons.

Kovda, I., and Mermut, A. R. (2018). "Vertic Features", in *Interpretation of Micromorphological Features of Soils and Regoliths*, eds. G. Stoops, V. Marcelino, and F. Mees (Amsterdam: Elsevier), 605–632.

Kovda, I., Morgun, E., and Boutton, T. W. (2010). Vertic processes and specificity of organic matter properties and distribution in Vertisols. *Eurasian Soil Sc*. 43, 1467–1476. doi: 10.1134/S1064229310130065

Kühn, P., Aguilar, J., Miedema, R., and Bronnikova, M. (2018). "Textural pedofeatures and related horizons", in *Interpretation of Micromorphological Features of Soils and Regoliths*, eds. G. Stoops, V. Marcelino, and F. Mees. (Amsterdam: Elsevier), 377–423.

Kvavadze, E., Boschian, G., Chichinadze, M., Gagoshidze, I., Gavagnin, K., Martkoplishvili, I., et al. (2019). Palynological and archaeological evidence for ritual use of wine in the Kura-Araxes Period at Aradetis Orgora (Georgia, Caucasus). *J. Field Archaeol.* 44, 500–522. doi: 10.1080/00934690.2019.1669254

Lewis, H. (2012). *Investigating ancient tillage: An Experimental and Soil Micromorphological Study, International Series*. Oxford: British Archaeological Reports.

Lilliu, G. (2004). *La Civiltà dei Sardi: dal Paleolitico all'età dei nuraghi*. Nuoro: Il Maestrale.

Limbrey, S. (1990). Edaphic opportunism? A discussion of soil factors in relation to the beginnings of plant husbandry in South-West Asia. *World Archaeol.* 22, 45–52. doi: 10.1080/00438243.1990.9980128

Lugliè, C. (2009). "L'obsidienne néolithique en Méditerranée Occidentale" in *L'Homme et le precieux. Matières Minérals Précieuses*, eds. M. H., Moncel, F. Frohlich (Oxford: British Archaeological Reports International Series), 213–224.

Lugliè, C. (2012). From the perspective of the source. Neolithic production and exchange of Monte Arci obsidians (central-western Sardinia). *Rubricatum* 5, 1135–3791.

Lugliè, C. (2018). Your path led trough the sea … The emergence of Neolithic in Sardinia and Corsica. *Q. Int.* 470, 285–300. doi: 10.1016/j.quaint.2017.12.032

Macphail, R. I., Courty, M.-., A., and Gebhardt, A. (1990). Soil micromorphological evidence of early agriculture in north-west Europe. *World Archaeology* 22, 53–69. doi: 10.1080/00438243.1990.9980129

Macphail, R. I., and Goldberg, P. (2018). *Applied soils and micromorphology in archaeology*. Cambridge: Cambridge University Press.

Matthews, W., French, C. A., Lawrence, T., Cutler, D. F., and Jones, M. K. (1997). Microstratigraphic traces of site formation processes and human activities. *World Archaeol.* 29, 281–308. doi: 10.1080/00438243.1997.9980378

Melis, M. G. (2013). "Problemi di cronologia insulare. La Sardegna tra il IV e il III millennio BC", in *Cronologia Assoluta E Relativa dell'età del rame in Italia (Atti dell'incontro di studi Universita di Verona, 25 June 2013*, eds. D. Cocchi-Genick. (Verona: QuiEdit), 197–211.

Melis, R. T., Rita, F. D., French, C., Marriner, N., Montis, F., Serreli, G., et al. (2018). 8000 years of coastal changes on a western Mediterranean island: a multiproxy approach from the Posada plain of Sardinia. *Marine Geol.* 403, 93–108. doi: 10.1016/j.margeo.2018.05.004

Miller, C. E., Conard, N. J., Goldberg, P., and Berna, F. (2010). Dumping, sweeping and trampling: experimental micromorphological analysis of anthropogenically modified combustion features. *Palethnologie* 2, 25–37. doi: 10.4000/palethnologie.8197

Nicosia, C., Langohr, R., Carmona Gonzalez, P., Gomez Bellard, C., Modrall, E. B., Ruíz Pérez, J. M., et al. (2013). Land use history and site formation processes at the Punic site of Pauli Stincus in west central Sardinia. *Geoarchaeology* 28, 373–393. doi: 10.1002/gea.21443

Nicosia, C., and Stoops, G. (2017). *Archaeological Soil and Sediment Micromorphology*. London: John Wiley and Sons.

Nielsen, N. H., and Dalsgaard, K. (2017). Dynamics of Celtic fields-A geoarchaeological investigation of Øster Lem Hede, Western Jutland, Denmark. *Geoarchaeology* 32, 414–434. doi: 10.1002/gea.21615

Nielsen, N. H., Kristiansen, S. M., Ljungberg, T., Enevold, R., and Løvschal, M. (2019). Low and variable: manuring intensity in Danish Celtic fields. *J. Archaeol. Sci. Rep.* 27, 101955. doi: 10.1016/j.jasrep.2019.101955

Pedrotta, T., Gobet, E., Schwörer, C., Beffa, G., Butz, C., Henne, P. D., et al. (2021). 8, 000. years of climate, vegetation, fire and land-use dynamics in the thermo-mediterranean vegetation belt of northern Sardinia (Italy). *Veget. Hist. Archaeobot.* 30, 789–813. doi: 10.1007/s00334-021-00832-3

Pinna, M. (1954). *Il clima della Sardegna*. Pisa: Libreria Goliardica.

Portillo, M., García-Suárez, A., Klimowicz, A., Barański, M. Z., and Matthews, W. (2019). Animal penning and open area activity at Neolithic Çatalhöyük, Turkey. *J. Anthropol. Archaeol.* 56, 101106. doi: 10.1016/j.jaa.2019.101106

Revelles, J., Ghilardi, M., Rossi, V., Currás, A., López-Bult,ó, O., Brkojewitsch, G., et al. (2019). Coastal landscape evolution of Corsica island (W. Mediterranean): paleoenvironments, vegetation history and human impacts since the early Neolithic period. *Q. Sci. Rev.* 225, 105993. doi: 10.1016/j.quascirev.2019.105993

Roberts, C. N., Woodbridge, J., Palmisano, A., Bevan, A., Fyfe, R., Shennan, S., et al. (2019). Mediterranean landscape change during the Holocene: synthesis, comparison and regional trends in population, land cover and climate. *The Holocene* 29, 923–937. doi: 10.1177/0959683619826697

Roberts, N. (2014). *The Holocene: An Environmental History*. London: John Wiley and Sons.

Robin, G., Soula, F., Tramoni, P., Lilley, K., Manca, L., Canu, N., et al. (2022). "Les relations spatiales entre nécropoles à hypogées et établissements de plein air en Sardaigne du 5e au 2e millénaire av. J.-C. : l'exemple de Mesu 'e Montes à Ossi", in *Sépultures et Rites Funéraires / Sepulture è Riti Funerari. Actes du Colloque Organisé par l'Association de Recherches Préhistoriques Corses (ARPPC) Calvi – 2019*, eds, J. Sicurani (Calvi: ARPPC), 79–97.

Santoni, V. (2000). "Alle origini dell'ipogeismo in Sardegna: Cabras-Cuccuru S'Arriu, la necropoli del Neolitico Medio" in *L'ipogeismo nel Mediterraneo: Origini, Sviluppo, Quadri Culturali. Atti del Congresso Internazionale, Sassari-Oristano 23-28 maggio 1994*, eds, J. Sicurani (Muros: Stampacolor), 369–397.

Scarciglia, F., Tuccimei, P., Vacca, A., Barca, D., Pulice, I., Salzano, R., et al. (2011). Soil genesis, morphodynamic processes and chronological implications in two soil transects of SE Sardinia, Italy: traditional pedological study coupled with laser ablation ICP-MS and radionuclide analyses. *Geoderma* 162, 39–64. doi: 10.1016/j.geoderma.2011.01.004

Sebis, S., Luglie, C., and Santoni, V. (2012). "Il Neolitico medio di Cuccuru is Arrius (Cabras, OR) nella struttura abitativa 422" in *Atti della XLIV Riunione Scientifica dell'Istituto Italiano di Preistoria e Protostoria La preistoria e la Protostoria Della Sardegna, Cagliari, Barumini, Sassari 23-28 novembre 2009, Volume II e Comunicazioni*, eds. C. Lugliè (Firenze: Istituto Italiano di Preistoria e Protostoria), 495–502.

Shahack-Gross, R. (2017). "Animal gathering enclosures," in *Archaeological Soil and Sediment Micromorphology*, eds. C. Nicosia and G. Stoops (New York, NY: Wiley-Blackwell), 265–280.

Shillito, L. M., Bull, I. D., Matthews, W., Almond, M. J., Williams, J. M., Evershed, R. P., et al. (2011). Biomolecular and micromorphological analysis of suspected fecal deposits at Neolithic Çatalhöyük, Turkey. *J. Archaeol. Sci.* 38, 1869–1877. doi: 10.1016/j.jas.2011.03.031

Shillito, L. M., and Matthews, W. (2013). Geoarchaeological investigations of midden-formation processes in the Early to Late Ceramic Neolithic Levels at Çatalhöyük, Turkey ca. 8550–8370 cal BP. *Geoarchaeology* 28, 25–49. doi: 10.1002/gea.21427

Spek, T., Waateringe, W. G., Kooistra, M., and Bakker, L. (2003). Formation and Land-Use History of Celtic Fields in North-West Europe – an Interdisciplinary Case Study at Zeijen, the Netherlands. *European Journal of Archaeology* 6, 141–173. doi: 10.1179/eja.2003.6.2.141

Stoops, G. (2003). *Guidelines for Analysis and Description of Soil and Regolith Thin Sections*. Madison, Wisconsin Soil Science Society of America, Inc.

Stoops, G., Marcelino, V., and Mees, F. (2018). *Interpretation of Micromorphological Features of Soils and Regoliths*. Amsterdam: Elsevier.

Thompson, M. L., Fedoroff, N., and Fournier, B. (1990). Morphological features related to agriculture and faunal activity in three loess-derived soils in France. *Geoderma* 46, 329–349. doi: 10.1016/0016-7061(90)90023-3

Ucchesu, M., Sau, S., and Lugliè, C. (2017). Crop and wild plant exploitation in Italy during the Neolithic period: New data from Su Mulinu Mannu, Middle Neolithic site of Sardinia. *J. Archaeol. Sci. Rep.* 14, 1–11. doi: 10.1016/j.jasrep.2017.05.026

Ulzega, A. (1999). "Lineamenti geomorfologici" in *Sardegna Paleolitica. Studi Sul più Antico Popolamento dell'isola*, eds. F. Martini (Firenze: Museo fiorentino di preistoria), 25–34.

Vacca, A., Serra, G., and Scalenghe, R. (2018). Vegetation, soils, and humus forms of Sardinian holm oak forests and approximated cross-harmonization of vegetation types,

WRB Soil Groups and humus forms in selected Mediterranean ecosystems. *Appl. Soil Ecol.* 123, 659–663. doi: 10.1016/j.apsoil.2017.06.024

Verrecchia, E. P., and Trombino, L. (2021). *A Visual Atlas for Soil Micromorphologists*. Cham: Springer International Publishing.

Vingiani, S., Righi, O., Petit, S., and Terribile, F. (2004). Mixed-layer kaolinite-smectite minerals in a red-black soil sequence from basalt in Sardinia (Italy). *Clays Clay Miner*. 52, 473–483. doi: 10.1346/CCMN.2004.0520408

Vita-Finzi, C. (1969). *Mediterranean valleys*. Cambridge: Cambridge University Press.

Wieder, M., and Yaalon, D. H. (1982). Micromorphological fabrics and developmental stages of carbonate nodular forms related to soil characteristics. *Geoderma* 28, 203–220. doi: 10.1016/0016-7061(82)90003-9

Williams, A. J., Pagliai, M., and Stoops, G. (2018). "Physical and Biological Surface Crusts and Seals", in *Interpretation of Micromorphological Features of Soils and Regoliths*, eds. G. Stoops, V. Marcelino, and F. Mees (Amsterdam: Elsevier), 539–574.

Yaalon, D. H. (1997). Soils in the Mediterranean region: what makes them different? *Catena* 28, 157–169. doi: 10.1016/S0341-8162(96)00035-5

Zucca, C., Vignozzi, N., Madrau, S., Dingil, M., Previtali, F., Kapur, S., et al. (2013). Shape and intraporosity of topsoil aggregates under maquis and pasture in the Mediteranean region. *J. Plant Nutr. Soil Sci.* 176, 529–539. doi: 10.1002/jpln.201200144